Systematic and Applied Microbiology 48 (2025) 126609

Contents lists available at ScienceDirect

Systematic and Applied Microbiology

journal homepage: www.elsevier.com/locate/syapm

N-glyceroyl alkylamine phosphoglycolipids dominate the lipidome of several Bacillota bacteria

Nicole J. Bale [a,*], Michel Koenen [a], Su Ding [a], Jaap S. Sinninghe Damsté [a,b,*]

[a] NIOZ Royal Institute for Sea Research, Department of Marine Microbiology and Biogeochemistry, Texel, the Netherlands
[b] Department of Earth Sciences, Faculty of Geosciences, Utrecht University, Utrecht, the Netherlands

ARTICLE INFO

Keywords:
Bacillota
Lipidome
N-glyceroyl alkylamine
Phosphoglycolipids
Membrane
Mass spectrometry

ABSTRACT

Elucidation of the membrane lipid composition of bacteria can help to better understand how bacterial cells interact with their surroundings, adapt to environmental stress, and resist antimicrobial agents. Here we describe for the first time the detection of a wide array of N-glyceroyl alkylamine phosphoglycolipids (NGAPs) in a range of *Bacillota* bacteria (formerly *Firmicutes*). *Bacillota* includes a diverse range of bacteria that are typically highly resistant to harsh conditions such as heat, radiation, and pH, allowing the bacteria to survive in unfavorable environments. In 9 out 18 investigated strains of *Bacillota*, spread across 5 orders (*Thermoanaerobacterales, Thermosediminibacterales, Eubacteriales, Halanaerobiales*, and *Sulfobacillia*) mild acid hydrolysis released N-glyceroyl alkylamines (NGAs), which were detectable by gas chromatography–mass spectrometry (GC–MS) during routine fatty acid analysis. One strain, *Moorella thermoacetica* was found to produce long-chain NGAs (C_{30}-C_{32}), which are postulated to have *iso*diabolic acid-like structures. A wide variety of intact polar NGAPs were identified using ultra-high pressure liquid chromatography high resolution multi-stage mass spectrometry (UHPLC-HRMS^n). These include many previously undescribed lipids with a variety of sugar moieties and glycerol-bound core lipid moieties, including ether-bound components and alkyl 1,2-diols. The NGAPs constituted the majority of the intact polar lipid composition of these strains and presumably contribute to their tough cell membranes. The presence of NGAs in *Bacillota* appears to be associated with thermophilia. Both the hydrolysis-derived NGAs and intact polar NGAPs have potential to be biomarkers for extremophilic and, in particular, thermophilic bacteria.

Introduction

Membrane lipids are the fundamental building blocks of cell walls and hence have a vital role in cell survival. To adapt to different environments, microorganisms have evolved diverse mechanisms to modify their membranes, adjusting the structure and proportions of specific lipids. The majority of bacterial membrane lipids are phospholipids, consisting of two fatty acids joined by a glycerol backbone, which also comprise a phosphate-based polar head group, such as phosphoglycerol, phosphoethanolamine or phosphocholine (see Sohlenkamp and Geiger, 2016 for a review). Structural adaptations of membrane lipids include changes in the acyl chains (fatty acids) as well as to their polar head groups. Lipid adaptation plays a key role in dealing with external environmental stressors such as temperature, pH, radiation and ion concentrations (e.g., Siliakus et al., 2017; Schubotz, 2019; Ding et al., 2024). However, not all bacteria have membranes composed of conventional phospholipids. For example, some bacteria possess a high abundance of ether lipids (Grossi et al., 2015; Sinninghe Damsté et al., 2023). Others replace phosphorus containing lipids with non-phosphorus lipids to adapt to specific nutrient scarcity (Geiger et al., 1999, 2010; Bosak et al., 2016; Ding et al., 2024). Certain bacteria produce membrane-spanning lipids (similar to those commonly produced by archaea) where they are thought to confer membrane stability (Clarke et al., 1980; Jung et al., 1994; Sinninghe Damsté et al., 2007, 2011; Sahonero-Canavesi et al., 2022a).

A limited number of extremophilic bacteria have been reported to have N-glyceroyl alkylamine phosphoglycolipids (NGAPs; cf. Fig. 1 for example structure). These lipids differ from classic phospholipids by the nature of their polar head groups. Like the majority of bacterial lipids, they have a 1,2-diacyl-glycero-3-phospho structure, however their head group moiety is based on an N-glyceroyl alkylamine (NGA) with a sugar moiety attached at the 3rd position (cf. Fig. 1) of the N-glyceroyl moiety

* Corresponding authors at: NIOZ Royal Institute for Sea Research, Department of Marine Microbiology and Biogeochemistry, Texel, the Netherlands.
E-mail address: nicole.bale@nioz.nl (N.J. Bale).

https://doi.org/10.1016/j.syapm.2025.126609
Received 19 February 2025; Received in revised form 29 April 2025; Accepted 30 April 2025
Available online 5 May 2025

(Anderson and Hansen, 1985; Huang and Anderson, 1989; Yang et al., 2006; Suda et al., 2012; Compton et al., 2020). These alkylamine lipids have been detected in *Deinococcus radiodurans* (Anderson, 1983; Anderson and Hansen, 1985; Huang and Anderson, 1989), other members of the *Thermus* and *Meiothermus* genera (Yang et al., 2006; Suda et al., 2012; Fujimoto et al., 2013; Lagutin et al., 2014), and *Chthonomonas calidirosea* of the *Armatimonadota* phylum (Compton et al., 2020). All these bacteria are extremophilic, in particular *D. radiodurans,* which is one of the most radiation-resistant organisms known (Cox and Battista, 2005). Interest in these compounds has been driven in part by their potential immunomodulatory function. It has been shown that this immunomodulatory activity is dependent on the chain lengths of the three acyl chains of the lipids (Gan et al., 2020) and that the stereo configuration of the diacyl glycerol moiety is important for immunostimulation (Fujimoto et al., 2013). Indeed, a mixture of two NGAPs, 2′-O-(1,2-diacyl-sn-glycero-3-phospho)-3′-O-(α-*N*-acetylglucosaminyl)-N-glyceroyl alkylamine and 2′-O-(2-acyl-alkyldio-1-O-phospho)-3′-O-(α-*N*-acetyl-glucosaminyl)-N-glyceroyl alkylamine isolated from *Meiothermus taiwanensis* and *Thermus oshimai* have been shown to up-regulate interleukin-1β (IL-1β; a cytokine protein) in human monocyte white blood cells (Yang et al., 2008). However, because they can form much of the total lipidome (approximately 43 % in *C. calidirosea*; Compton et al., 2020), they must also function as membrane lipids.

Here we describe for the first time the detection using ultra-high pressure liquid chromatography high resolution multi-stage mass spectrometry (UHPLC-HRMS^n) of a wide range of NGA phosphoglycolipids (NGAPs) in a suite of *Bacillota* bacteria (formerly *Firmicutes*). We found that NGAPs constituted up to 78 % of the polar lipid extracts of these strains and include many previously undescribed lipids. The *Bacillota* is a large taxonomic group that includes a diverse range of bacteria that are typically rod-shaped and have the ability to form dormant endospores, which are highly resistant to harsh conditions such as heat, radiation, and chemicals, allowing them to survive in unfavorable environments (Filippidou et al., 2016).

Methods

Bacterial strains

All cultures (Table 1), except *Thermoanaerobacter ethanolicus*, were grown at DSMZ in 0.5 or 1 l Erlenmeyer flasks at standard conditions and were harvested in the transit of the late exponential phase to the beginning stationary phase. The cells of all strains were harvested by centrifugation in either the Sorvall RC 6plus centrifuge (rotor F109-6x500y) at 9000 rpm for 20 min or in the Beckman coulter centrifuge Avanti® J-30I (rotor JA-14; Galway, IRE) at 10000 rpm for 20 min. After the liquid was removed the harvested cells were lyophilized overnight in a freeze-drying machine Christ Alpha 1–4 LDplus (Osterode am Harz, GER) at −60 °C and 0.025 mbar. *T. ethanolicus* was grown and harvested as described earlier (Sahonero-Canavesi et al., 2022a).

Lipid extraction and analysis

For hydrolysis-derived lipid analysis, freeze-dried biomass was hydrolyzed by mild acid reflux with 1.4 N HCl in methanol (MeOH) for 3 h. Such acid hydrolysis converts ester-bound lipids into fatty acids and glycosidic bound-lipids into alcohols, while ether bonds remain unaffected. Amide bound-fatty acids can also be hydrolyzed with acid reflux, however this reaction is much slower than that of ester-bound fatty acids. After neutralization with a 2 N KOH/MeOH (1/1, *v*/v), the fatty acids were methylated with diazomethane in diethyl ether, which was removed under a stream of N_2. Before analysis the extracts were treated with pyridine (10 µl) and *N*,*O*-bis(trimethylsilyl)trifluoroacetamide (BSTFA, 10 µl) to derivatize alcohol groups and were brought to a final volume with ethyl acetate to a concentration of 1 mg ml^{-1}. Hydrolysis-derived lipid quantification was carried out on an Agilent 7890B gas chromatograph (GC; Agilent, Santa Clara, CA, United States) with an Agilent CP Sil-5 silica column (25 × 0.32 mm) and helium as the carrier gas at a constant flow rate of 2 ml min^{-1}. The oven temperature program initiated at 70 °C, then increased, first at a rate of 20 °C min^{-1} to 130 °C, and next at a rate of 4 °C min^{-1} to the final temperature of 320 °C, which was held for 10 mins. FAME identification was carried out on an Agilent 7890 A GC coupled to an Agilent 5975C VL MSD mass spectrometer (MS) operated at 70 eV, with a mass range *m/z* 50–800 and 3 scans per second. The column and oven settings were the same as for the quantification GC analysis. Hydrolysis-derived lipids were identified based on literature data and library mass spectra. Double bond positions were determined using dimethyldisulfide (DMDS) derivatization of the lipids as described previously (Bale et al., 2019). Quantification and identification were as per (Bale et al., 2019) and compounds were identified based on literature data and library mass spectra. To identify the NGAs, analysis was repeated with deuterated BSTFA (3 µl) to derivatize alcohol groups.

Intact polar lipids (IPLs) were extracted from freeze-dried biomass using a modified Bligh–Dyer procedure and analyzed by reverse phase UHPLC-HRMS^n (Bale et al., 2021). An Agilent 1290 Infinity I UHPLC, equipped with thermostatted auto-injector and column oven, coupled to a Q Exactive Orbitrap mass spectrometer with an Ion Max source with a heated electrospray ionization probe (Thermo Fisher Scientific) was used. IPLs were separated on an Acquity BEH C_{18} column (Waters, 2.1 × 150 mm, 1.7 µm), maintained at 30 °C, using a flow rate of 0.2 ml min^{-1}. For this separation a mixture of two different eluents was used; eluent A was composed of a mixture of methanol and H_2O (85:15, v:v) and eluent B of methanol and *iso*propanol (50:50, v:v). Both eluents were modified by addition of small amounts of formic acid (0.12 %, *v*/v) and 14.8 M NH3aq (0.04 %, v/v). The elution program was as follows: 95 % A for 3

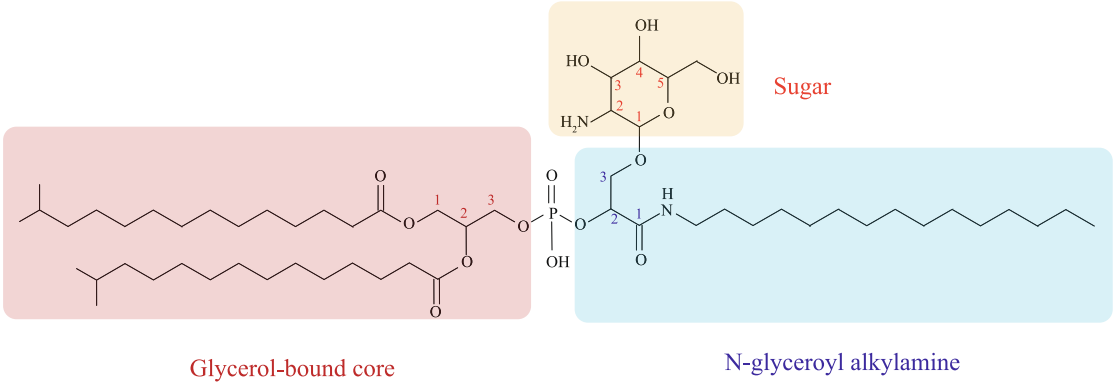

Fig. 1. Example structure of a N-glyceroyl alkylamine phosphoglycolipid (NGAP) with a diacyl glycerol (DAG) core with 30 non-glycerol carbons (drawn as two *iso*-C_{15} fatty acids). The sugar is glucosamine and the alkylamine is *n*-C_{15}.

Table 1
The taxonomy, Gram stain, temperature growth range and physiology of the anaerobic *Bacillota* strains analyzed. The presence of N-glyceroyl alkylamines (NGAs), as detected by GC–MS, at the cultivation temperature listed is indicated.

Class	Order	Strain	DSM No.	Gram stain	Growth range (°C)[a]	Physiology	Lit.[b]	Cult. T (°C)	NGAs
Clostridia	*Thermoanaero-bacterales*	*Caldanaerobacter subterraneus* OCA1	15729	+	**40–75**	acetogenic sugar fermenter, thiosulfate-reducer	1	70	✓
		Caldicellulosiruptor owensensis OL^T	13100	–	**50–80**	sugar fermenter	2	70	–
		Moorella thermoacetica ET-5a	12797	+	**36–70**	acetogen	3	55	✓
		Thermoanaerobacter ethanolicus JW200^T	2246	+	**37–78**	sugar fermenter	4	65	✓
		Thermoanaerobacter wiegelii Rt8.B1^T	10319	–	**38–78**	sugar fermenter	5	65	✓
	Thermosedimini-bacterales	*Fervidicola ferrireducens* Y170^T	21121	–	**55–80**	sugar fermenter	6	70	✓
		Thermosediminibacter oceani JW/IW-1228P^T	16646	–	**52–76**	sugar fermenter, thiosulfate- and S_8-reducer	7	65	✓
		Acetobacterium woodii WB1^T	1030	+	30	H_2-oxidizing, CO_2-reducing acetogen	8	30	–
		Alkaliphilus transvaalensis SAGM1^T	29504	+	20–50	alkaliphilic chemoorganotroph	9	30	–
		Clostridium magnum Thai5A-GV	13769	–	15–45	acetogen	10	30	–
	Eubacteriales	*Desulfoscipio gibsoniae* Groll^T	7213	+	20–40	sulfate-reducer	11	35	✓
		Desulfosporosinus orientis Ulu Singapore II	7439	+	30–42	sulfate-reducer	12	30	–
		Oscillibacter valericigenes Sjm 18-20^T	18026	–	15–35	valeric acid-producing sugar fermenter	13	30	–
		Halanaerobium congolense SEBR 4224^T	11287	–	20–45	moderately halophilic thiosulfate- and S_8-reducer	17	40	–
	Halanaerobiales	*Halanaerobium lacusrosei* H 200^T	10165	–	20–50	halophilic fermenter	16	37	–
		Halanaerobium saccharolyticum Z-7787^T	6643	–	15–47	halophilic sugar fermenter	15	37	–
		Halocella cellulosilytica Z-10151^T	7362	–	20–50	halophilic cellulose degrader	14	37	✓
Sulfo-bacillia	*Sulfobacillales*	*Sulfobacillus thermosulfidooxidans* 41^T	11920	+	**20–60**	acidophilic, S oxidizer	18	50	✓

[a] Growth range for thermophiles is indicated in bold.
[b] (1) (Fardeau et al. (2004); (2) Huang et al. (1998); (3) Wiegel et al. (1981); (4) Wiegel and Ljungdahl (1981); (5) Cook et al. (1996); (6) Ogg and Patel (2009); (7) Lee et al. (2005); (8) Balch et al. (1977); (9) Takai et al. (2001); (10) Schink (1984) (11) Kuever et al. (1999); (12) Campbell and Postgate (1965); (13) Iino et al. (2007); (14) Ravot et al. (1997); (15) Cayol et al. (1995); (16) Rainey et al. (1995); (17) Simankova et al. (1993); (18) Golovacheva and Karavaĭko (1978).

min, followed by a linear gradient to 40 % A at 12 min and then to 0 % A at 50 min. These latter conditions were maintained until 80 min. The settings for the electrospray ionization probe, operated in positive ion mode, were: capillary temperature, 300 °C; sheath gas (N_2) pressure, 40 arbitrary units (AU); auxiliary gas (N_2) pressure, 10 AU; spray voltage, 4.5 kV; probe heater temperature, 50 °C; S-lens 70 V. The Q Exactive mass spectrometer was calibrated within a mass accuracy range of 1 ppm using the Thermo Scientific Pierce LTQ Velos ESI Positive Ion Calibration Solution. The IPLs were analyzed with a mass range of *m/z* 350–2000 with a resolving power of 70,000 ppm at *m/z* 200. Data-dependent tandem MS/MS (resolving power 17,500 ppm) was successively performed by fragmentation of the 10 most abundant ions (stepped normalized collision energy 15, 22.5, 30; isolation width, 1.0 *m/z*). Dynamic exclusion was used to temporarily exclude masses (for 6 s) to allow selection of less abundant ions for MS/MS. Note that IPLs have varying degrees of ionization efficiency. Hence, the peak areas (in response units) of different IPLs do not necessarily reflect their actual relative abundance. However, this method allows for comparison between samples when analyzed in the same batch.

Results

As part of the Microlipids research program, which is striving to systematically characterize prokaryotic intact polar lipids with state-of-the-art analytical techniques, we examined the hydrolysis-derived lipid composition of 18 strains of *Bacillota* (Table 1), a phylum previously known as *Firmicutes*. Of the 18 strains, 17 were from the class *Clostridia*, spread across 4 orders: *Thermoanaerobacterales, Thermosedimini**bacterales, Eubacteriales* and *Halanaerobiales*. The final strain, *Sulfobacillus thermosulfidooxidans,* was from the class *Sulfobacillales* and order *Sulfobacillia*.

Common hydrolysis-derived lipids

A wide range of hydrolysis-derived lipids were detected across the 18 *Bacillota* strains through mild acid hydrolysis of freeze-dried biomass (Fig. 2A; Table S1). The strains contained fatty acids, hydroxy fatty acids, membrane-spanning dicarboxylic acids (such as isodiabolic acid, cf. (Jung et al., 1994; Sinninghe Damsté et al., 2018)), dimethylacetals (DMAs; formed upon acid hydrolysis from ether lipids containing an alk-1-enyl ether substituent at the *sn*-1 carbon of glycerol, so called plasmalogens (Goldfine, 2022)), and mono alkyl glycerol (derived from non-plasmalogen monoether lipids). The strains also contained varying amounts of alkyl 1,2-diols, wax esters and alcohols (Fig. 2A; Table S1).

Unusual hydrolysis-derived lipids

Additionally, nine of the investigated strains contained unusual lipids with a shared mass spectral fragmentation pattern. Eleven of these were detected in total and they eluted after the majority of the common hydrolysis-derived lipids (e.g., Fig. 3a); the first 8 compounds (A-H; Fig. 3) in the range ~ 25–35 min, while the other three (I—K) eluted later still, in the range ~ 47–50 min (cf. Fig. 3b). In total these 11 compounds accounted for up to ca. 16 % of the hydrolysis-derived lipids in one species (*M. thermoacetica*) (Table S1, Fig. 2).

The mass spectra of compounds A – H showed odd molecular ions at *m/z* 445, 459, 471, 473 and 487 in contrast to the much more common even molecular ions (e.g., Fig. 4a), suggesting that they contained one N atom. Losses from the molecular ions included 15, 30, 90 Da (e.g. for compound D, Fig. 4a). We assigned the loss of 15 Da as CH_3, 30 Da as 2× CH_3 and 90 Da as HO-Si$(CH_3)_3$, indicating the presence of a silylated hydroxy group. A characteristic fragment was observed at *m/z* 205 in all mass spectra, which suggests the presence of two adjacent carbon atoms, each bearing a silylated hydroxy group. To confirm whether the *m/z* 205

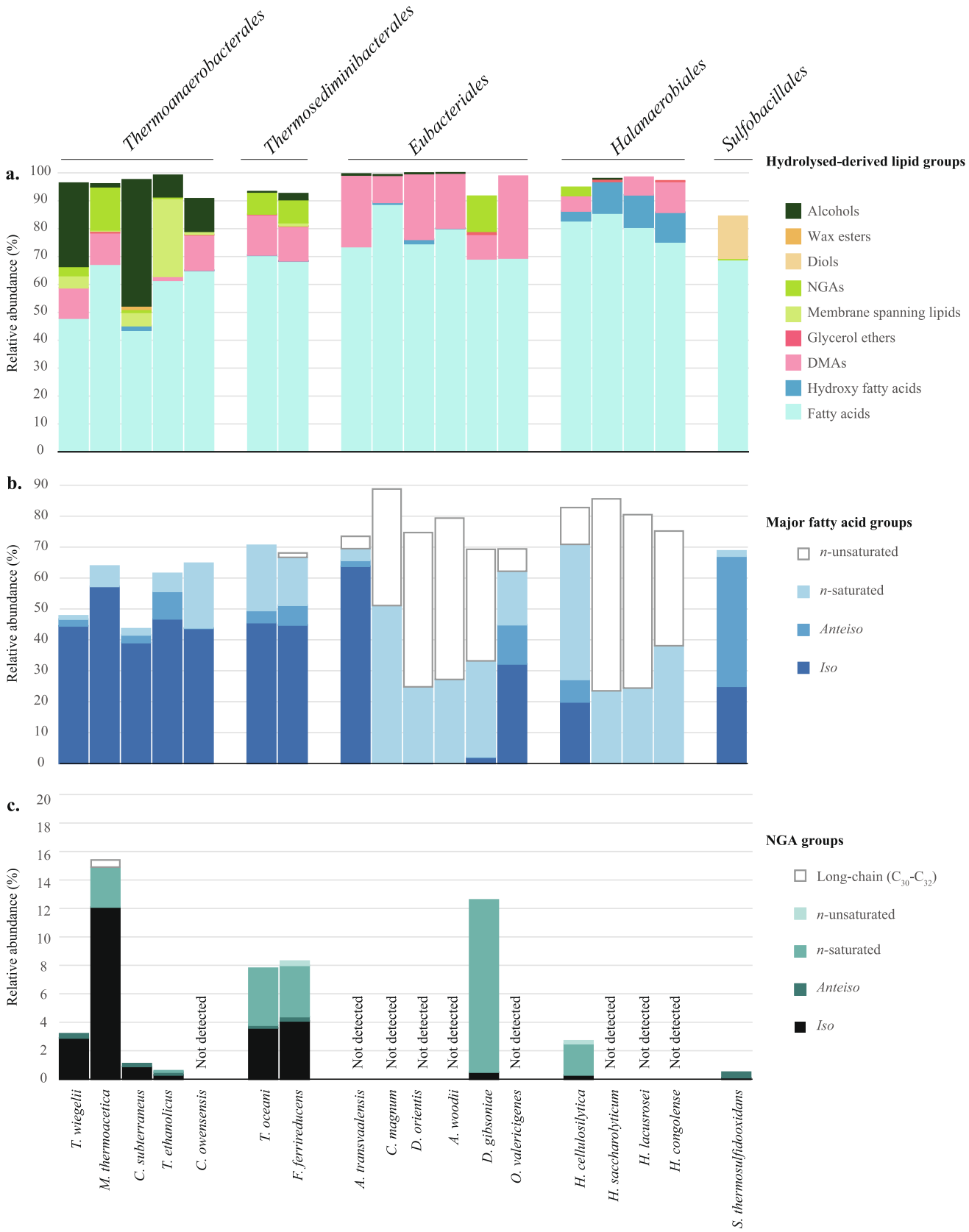

Fig. 2. Hydrolysis-derived lipid distribution across the 18 investigated strains of *Bacillota*. a) Hydrolysis-derived lipids distribution (by groups), b) fatty acids by groups, and c) NGA distribution by groups. For the full distribution of hydrolysis-derived lipids see Table S1. Values do not reach 100 because compounds were excluded if not present at a relative abundance >0.5 % in at least one strain (with the exception of long-chain NGAs) as are the unknown lipids.

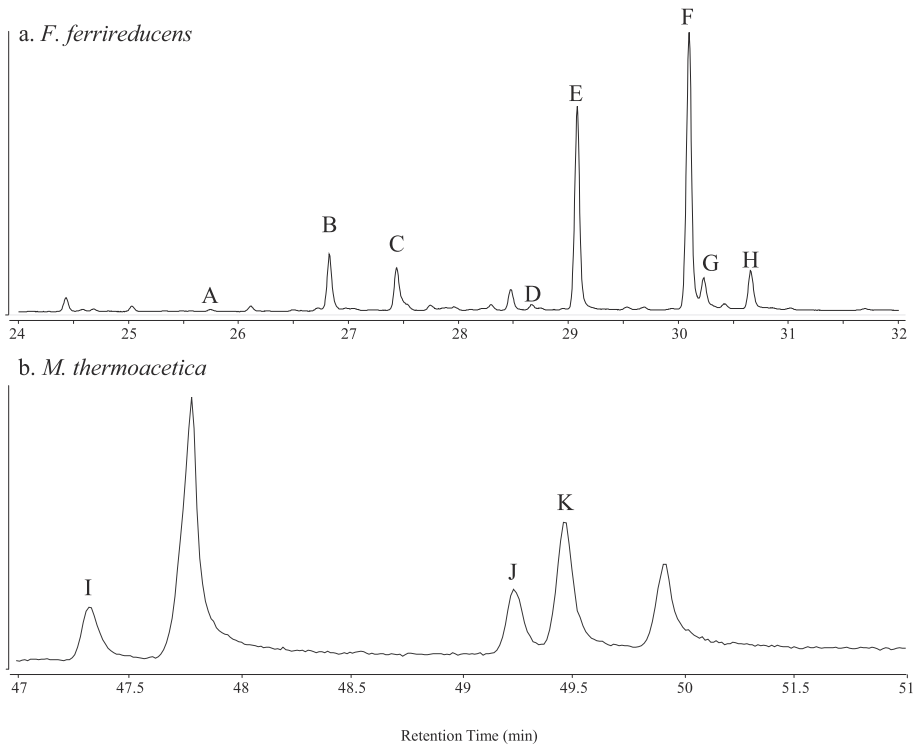

Fig. 3. Partial total ion chromatograms of the acid hydrolyzed biomass of (a) *F. ferrireducens* and (b) *M. thermoacetica*. Labels of N-glyceroyl alkylamines: A = *n*-$C_{14:0}$; B = *iso*-$C_{15:0}$; C = *n*-$C_{15:0}$; D = *n*-$C_{16:1}$; E = *n*-$C_{16:0}$; F = *iso*-$C_{17:0}$; G = *anteiso*-$C_{17:0}$; H = *n*-$C_{17:0}$; I = $C_{30:0}$ *iso*-diabolic acid-like; J = $C_{31:0}$; K = $C_{32:0}$ *iso*-diabolic acid-like.

fragment was indeed derived from a silylated ethyl-1,2-diol moiety, an aliquot of the hydrolyzed extract was derivatized with deuterated BSTFA. The silylated *m/z* 205 fragment was now detected at *m/z* 223 (a shift of 18 Da), confirming that the fragment contained two OTMS groups. In the case of the molecular ion at *m/z* 459, deuterated silylation led to a molecular ion at *m/z* 477 (Fig. 4b), an increase in 18 Da, confirming the presence of two OTMS groups, and by extension two adjacent hydroxy groups. On searching of the literature, a suite of membrane lipids was found that were comprised of two adjacent hydroxy groups and a nitrogen atom: NGAs, present in a range of extremophilic bacteria (Anderson and Hansen, 1985; Huang and Anderson, 1989; Yang et al., 2006; Suda et al., 2012; Compton et al., 2020). As NGAs have previously been described in *D. radiodurans* (Anderson, 1983; Anderson and Hansen, 1985; Huang and Anderson, 1989), we analyzed the hydrolysis-dervived lipids of *D. radiodurans* in the same way as for the *Bacillota* strains. Analysis by GC–MS confirmed identical spectra and retention times to those of the late-eluting compounds (e.g. Fig. 4c), confirming their assignment as a series of NGAs.

A second series, composed of three larger, NGAs (compounds I – K), was detected in *M. thermoacetica*, but not in any of the other bacteria studied (Table S1). They also possessed odd molecular ions but at much higher *m/z* values, namely at *m/z* 713, 727, and 741 (Fig. 5). They also exhibited losses from the molecular ion of 15, 30, 90 Da (e.g. Fig. 5), which we assigned in an identical manner as for the NGAs A - H, indicating a silylated hydroxy group and they also contained the unusual fragment at *m/z* 205 indicative of two adjacent silylated hydroxy moieties. Based on these spectral characteristics, and the presence of $C_{30:0}$ *iso*diabolic acid in *M. thermoacetica* (cf. membrane spanning lipids in Table S1), we assigned compounds I – K as silyl- and methyl-derivatized NGAs with C_{30}-C_{32} *iso*diabolic acid-like structures, as shown in Fig. 5.

Hydrolysis-derived lipid distribution

The acid hydrolysis-derived lipid distribution (also commonly referred to as core lipids) among the 18 *Bacillota* strains was relatively specific for each of the 5 orders (Fig. 2). The hydrolysis-derived lipid distribution of the five members of the *Thermoanaerobacterales* were characterized by higher levels of alcohols and membrane-spanning lipids (Fig. 2A), in particular in *T. ethanolicus*, where the $C_{30:0}$ *iso*-diabolic acid (Sinninghe Damsté et al., 2011) constituted 24 % of the acid hydrolysate. The fatty acids were mostly *iso*-fatty acids (Fig. 2b), with *iso*-$C_{15:0}$ and *iso*-$C_{17:0}$ particularly high (Fig. 2b; Table S1). All but *C. owensensis* contained NGAs (Fig. 2c), most noticeably in *M. thermoacetica* (i.e., 16 % of total hydrolysis-derived lipids, Table S1). The alkyl chain of the alkylamines were also mostly also *iso*- alkylamines. *M. thermoacetica* also contained three long-chain C_{30} – C_{32} NGAs (Fig. 5), which were not detected in any of the other strains.

The hydrolysis-derived lipid distributions of the two members of the *Thermosediminibacterales* were relatively similar to those of the *Thermoanaerobacterales*. They both contained dimethylacetals (formed upon acid hydrolysis of plasmalogen lipids) and hydroxy fatty acids (Fig. 2A). They contained more straight-chain saturated fatty acids than the *Thermoanaerobacterales*, in particular *n*-$C_{16:0}$ (Fig. 2b; Table S1). Both *Thermosediminibacterales* strains contained NGAs, particularly in *iso* and straight-chain saturated form (Fig. 2c).

The six strains from the *Eubacteriales* order also exhibited uniformity in their hydrolysis-derived lipid distribution (Fig. 2). This order was characterized by higher levels of dimethylacetals (indicative of plasmalogen lipids; Fig. 2a). In 4 of the 6 species of this order the most dominant fatty acids were straight-chain unsaturated fatty acids (Fig. 2b), in particular *n*-$C_{14:0}$, *n*-$C_{16:1}$ (with various positions for the double bond) and *n*-$C_{16:0}$ (Table S1). Two strains contained high levels of branched fatty acids, in particular *iso*-$C_{15:0}$. Only one of the six *Eubacteriales* strains in this order contained the NGAs, *D. gibsoniae*, where they constituted up to ca. 15 % of the total hydrolysis-derived lipids (Fig. 1C).

The four strains from the *Halanaerobiales* had hydrolysis-derived lipid distributions quite distinct from those of the other orders (Fig. 2a). Two of the four species contained low levels (<1 %) of alkyl glycerol monoethers indicative of mixed ether/ester lipids without a

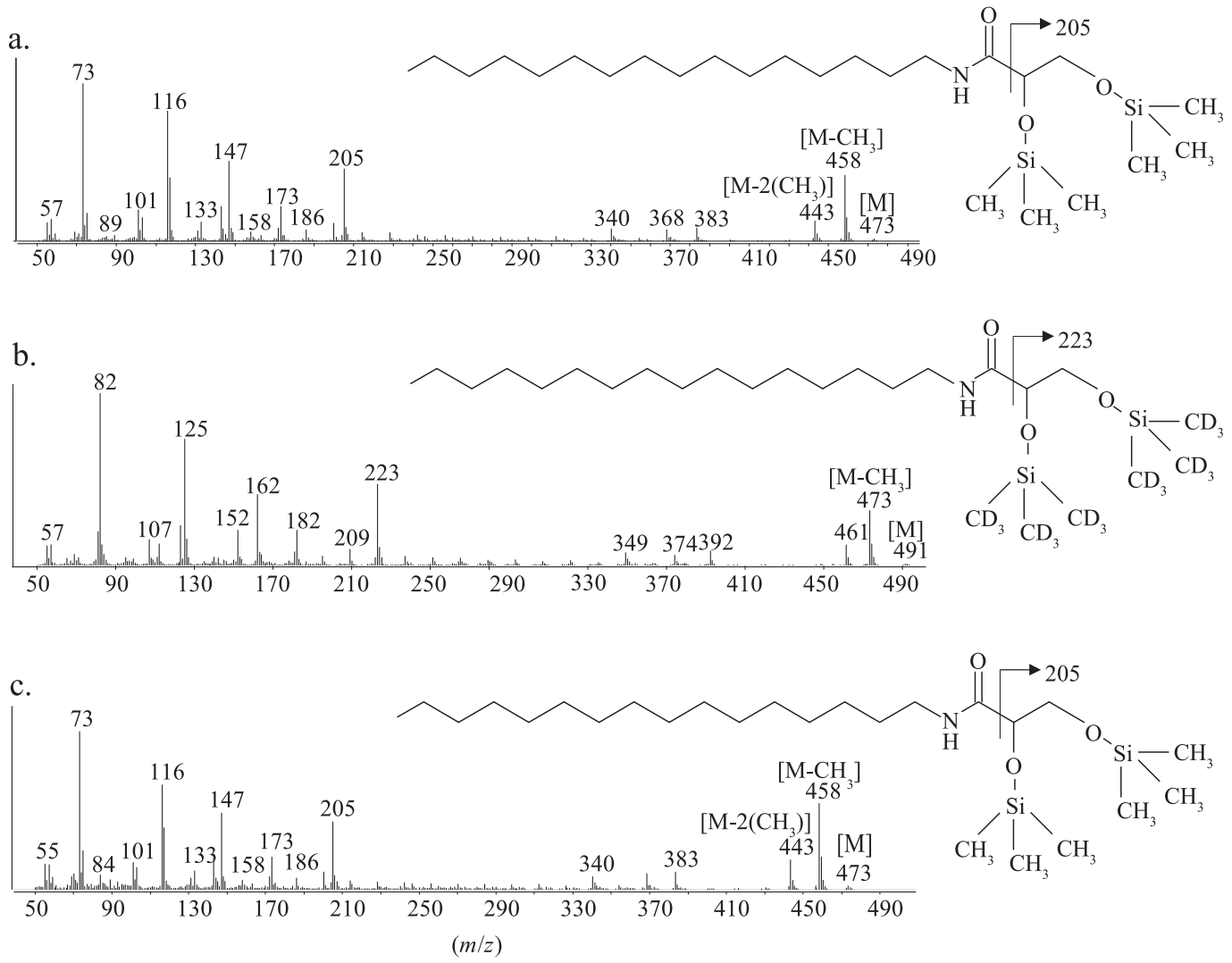

Fig. 4. Mass spectra of a) compound D in the acid hydrolysed, freeze-dried biomass of *F. ferrireducens*, b) compound D from *F. ferrireducens* using deuterated silylation and c) *N*-acetyl-16:0-alkylamine from acid hydrolyzed freeze-dried biomass of *D. radiodurans*.

double bond in the vicinal position of the ether linkage (Fig. 2a). The species of this order was also characterized by the absence of membrane-spanning lipids (Fig. 2a). The most dominant fatty acids in these strains were straight-chain unsaturated ones (Fig. 2b), in particular *n*-$C_{15:1}$ and *n*-$C_{16:1}$ (both with various positions of the double bond; Table S1). Only one of the four strains from the *Halanaerobiales* order contained NGAs, *H. cellulosilytica*, (up to ca. 3 % of the total; Fig. 2, Table S1).

Finally, the strain *S. thermosulfidooxidans*, was the only strain not falling in the *Clostridia* class, being from the class *Sulfobacillia* and order *Sulfobacillales*. This strain had the distinction of containing C_{16}-C_{18} alkyl 1,2-diols (Fig. 2a, Table S1). Its fatty acid composition was characterized by *anteiso*-fatty acids (Fig. 2b), in particular *anteiso*-$C_{15:0}$ and *anteiso*-$C_{17:0}$ (Fig. 2b). This contrasts with the other strains where branched fatty acids were always dominated by *iso*-fatty acids (Fig. 2b), although *S. thermosulfidooxidans* also contained a high proportion (16.5 %) of the *iso*-$C_{16:0}$ fatty acid (Table S1). This strain did contain hydroxy fatty acids, but no ether lipids. It only contained trace levels (<1 %) of NGAs (Fig. 2c).

Identification of intact NGA phosphoglycolipids

We examined the IPL composition of eight of the *Bacillota* strains that contained NGAs in detail by UHPLC-HRMS^n (Table 2, for expanded information see Table S2). NGAPs represented between 20 and 80 % of the total peak area of the base peak chromatogram (Table 2). Very few commonly occurring bacterial polar lipids were detected in the strains, apart from low levels of cardiolipins and quinones (data not shown). The NGAPs were identified based on their accurate masses and their fragmentation under MS^2 (cf. Figs. 7–9 for example MS^2 spectra and postulated structures and Supplementary Figs. S1–5 for further examples of MS^2 spectra). These mass spectra provided information on the sugar moiety, the glycerol-bound core moiety (e.g. a diacylglycerol) and individual fatty acids. The NGA moieties of the NGAPs were not observed as specific fragment ions in the MS^2 spectra of the NGAPs. Instead, they were either observed as a larger fragment ion (e.g., the ion at *m/z* 585.351 in Fig. 6) or determined from the accurate mass of the parent ion, after deduction of the sugar and the glycerol-bound core moieties.

The majority of the sugar moieties were either an *N*-acetylglucosamine, as revealed by an *m/z* 204.087 fragment ion in their MS^2 spectra (e.g., Fig. 7), a glucosamine sugar as revealed by a *m/z* 162.076 fragment ion (e.g., Fig. 6), or a hexose sugar (not observable as a fragment ion but as part of a loss; e.g., see MS^2 spectrum Fig. S3). *M. thermoacetica* also contained NGAPs with an unusual N-containing sugar, which gave rise to a distinctive ion in MS^2 at *m/z* 247.128 (Fig. S1), corresponding to an elemental composition of $C_{10}H_{19}O_5N_2$. Similarly, *T. wiegelii* and

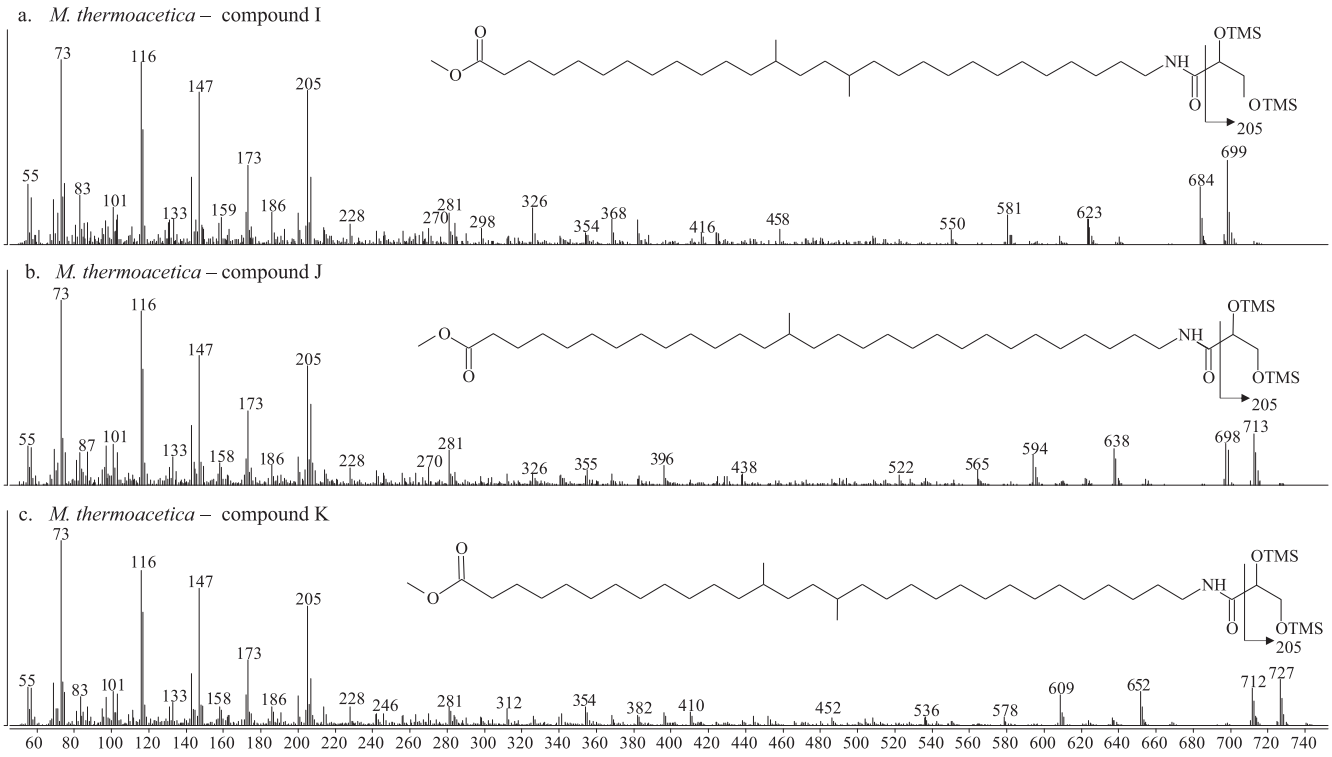

Fig. 5. a-c) Mass spectra of NGAs I – K in the acid hydrolyzed, freeze-dried biomass of *M. thermoacetica.* Labels of NGAs: I = $C_{30:0}$ *iso*-diabolic acid-like; J = $C_{31:0}$; K = $C_{32:0}$ *iso*-diabolic acid-like.

C. subterraneus contained NGAPs with an N-containing sugar, which gave rise to a fragment ion in MS^2 at *m/z* 233.113 (MS^2 spectrum Fig. S2), corresponding to an elemental composition of $C_9H_{17}N_2O_5$. With the assumption that these two sugar moieties fragmented from the parent ion via cleavage of the C1 – O bond (cf. numbering of carbon at in Fig. 1), as per the other sugars (cf. Figs. 7–8), these two sugars were assigned as having a molecular formula of $C_{10}H_{20}N_2O_6$ and $C_9H_{18}N_2O_6$, respectively. On close examination of the MS^2 spectra associated with the compounds bearing the $C_{10}H_{20}N_2O_6$ sugar (cf. Fig. S1), it was noted the presence of a glucosamine sugar fragment at *m/z* 162.076 ($C_6H_{12}O_4N$), indicating that the $C_{10}H_{19}N_2O_5$ ion underwent loss of a $C_3H_7O_2N$ neutral fragment (85.052 Da). Similarly, the $C_9H_{17}O_5N_2$ sugar ion (cf. Fig. S2) underwent loss of a C_4H_7ON neutral fragment (89.047 Da) resulting in a smaller sugar fragment ion at *m/z* 144.065 ($C_6H_{10}O_2N$). The complete structure of these sugars could not be determined at this time. It is possible that these may be similar to bacilliosamine, a sugar that was first isolated from *Bacillus subtilis* (Sharon, 1957, 2007), belonging to the *Bacillota,* but further work would be necessary to determine their structures.

The majority of the NGAP MS^2 spectra contained a dominant ion which was either associated with a diacyl glycerol (DAG) core (cf. MS^2 spectrum Fig. 6) or an acyl/ether glycerol (AEG) core (cf. MS^2 spectrum Fig. 7). These fragment ions are commonly observed in the MS^2 spectra of IPLs (Sturt et al., 2004) and can be distinguished by their accurate masses, which reveal the number of oxygen atoms present (i.e. four atoms for DAG and three for AEG). In the case of *S. thermosulfidooxidans* a series of NGAPs were detected which gave rise to MS^2 spectra that contained a dominant fragment ion containing only 2 oxygen atoms (cf. MS^2 spectrum Fig. 8). While some bacteria produce lipids with a diether glycerol (DEG) core (e.g. Hamilton-Brehm et al., 2013; Grossi et al., 2015; Krake et al., 2022; Ding et al., 2024) this could not be the case for *S. thermosulfidooxidans*, as acid hydrolysis did not produce any ether bound lipids (Table S1). Rather, the acid hydrolysis-derived lipid distribution of *S. thermosulfidooxidans* was characterized by the presence of alkyl 1,2-diols (Fig. 2a; Table S1), not seen in any of the other strains. Indeed, these constituted ca. 15 % of the hydrolysis-derived lipids for this strain. Hence, we postulated that several of the NGAPs detected in *S. thermosulfidooxidans* contained a core based on an alkyl 1,2-diol bound to a fatty acid (cf. MS^2 spectrum Fig. 8) as has been seen in other NGAPs producing bacteria such as *M. ruber* (Yang et al., 2006; Lin et al., 2013; Lagutin et al., 2014).

Present only in *C. subterraneus* (Table 2) are a number of compounds postulated to contain glyceroyl alkyls rather than NGAs (Fig. S4 for example mass spectrum and Fig. 6 for comparison with an analogous NGAP). During GC–MS analysis, *M. thermoacetica* was found to contain three long-chain (C_{30} – C_{32}) NGAs, not present in any other strain (Fig. 5 and Table S1). During IPL analysis a number of compounds gave rise to MS^2 spectra, which contained a fragment assigned as a long-chain alkylamine with a carboxylic acid group at the end (e.g. Fig. 9). The spectral evidence points towards phosphoglycolipids with long-chain NGA moieties. These possess the same sugars as the NGAP with C_{15}–C_{17} NGA moieties (cf. Fig. 9). The *m/z* values of the $[M + H]^+$ ions between 1091.785 and 1162.822 (Table 2) indicate that the acylglycerol moiety is probably in a lyso form (in which one of the fatty acids is not present). Due to the novel nature of the compounds, the postulated structure given in Fig. 9 is tentative. In order to assign a confirmed structure to these compounds one would need to isolate the compounds and carry out further structural analysis.

Distribution and composition of NGAPs

The NGAPs varied in the composition of the sugar moiety (Table 2), the majority being an *N*-acetylglucosamine as previously detected in thermophilic bacteria of the *Thermus* and *Meiothermus* genera (Yang et al., 2006). Five strains, *M. thermoacetica*, *C. subterraneus*, *T. oceani*, *F. ferrireducens* and *S. thermosulfidooxidans* also contained NGAPs with a glucosamine sugar, generally in lower proportions than those with a *N*-acetylglucosamine sugar. *M. thermoacetica* also contained NGAPs with an unusual N-containing sugar, with elemental composition of $C_{10}H_{19}O_5N_2$. Similarly, *T. wiegelii* and *C. subterraneus* contained N-

Table 2
Intact polar N-glyceroyl alkylamine phosphoglycolipids (NGAPs) and closely related compounds, detected by UHPLC-HRMS^n across 8 strains of *Bacillota*.

	Mass (obs)	Mass (calc)	Δmmu	AEC	RT (min)	Sugar	Alkylamine†	Core	%BPC
T. wiegeli	1093.763	1093.764	−1.0	$C_{57}H_{110}O_{15}N_2P$	22.6	*N*-acetylglucosamine	C_{17}	DAG $C_{26:0}$	1.2
	1105.801	1105.800	1.0	$C_{59}H_{114}O_{14}N_2P$	26.5	*N*-acetylglucosamine	C_{15}	AEG $C_{30:1}$	3.4
	1121.795	1121.795	0.0	$C_{59}H_{114}O_{15}N_2P$	24.9	*N*-acetylglucosamine	C_{15}	DAG $C_{30:0}$	0.5
	1133.832[a]	1133.832	0.0	$C_{61}H_{118}O_{14}N_2P$	28.8	*N*-acetylglucosamine	C_{17}	AEG $C_{30:1}$	10.2
	1135.811	1135.812	−1.0	$C_{57}H_{110}O_{15}N_2P$	26.7	*N*-acetylglucosamine	C_{17}	DAG $C_{29:0}$	2.7
	1149.826	1149.826	0.0	$C_{61}H_{118}O_{15}N_2P$	27.4	*N*-acetylglucosamine	$C_{15/17}$	DAG $C_{30:0}/C_{32:0}$	8.9
	1161.863	1161.863	0.0	$C_{63}H_{122}O_{14}N_2P$	31.5	*N*-acetylglucosamine	C_{17}	AEG $C_{32:1}$	8.6
	1162.858	1162.858	0.0	$C_{62}H_{121}O_{14}N_3P$	34.5	*m/z* 233 - $C_9H_{17}O_5N_2$	C_{17}	AEG $C_{30:1}$	4.3
	1177.857	1177.858	−1.0	$C_{63}H_{122}O_{15}N_2P$	30.2	*N*-acetylglucosamine	C_{17}	DAG $C_{32:0}$	10.2
	1178.854[b]	1178.853	1.0	$C_{62}H_{121}O_{15}N_3P$	32.7	*m/z* 233 - $C_9H_{17}O_5N_2$	C_{17}	DAG $C_{30:0}$	4.2
	1190.889	1190.889	0.0	$C_{64}H_{125}O_{14}N_3P$	37.3	*m/z* 233 - $C_9H_{17}O_5N_2$	C_{17}	AEG $C_{32:1}$	3.5
	1206.884	1206.884	0.0	$C_{64}H_{125}O_{15}N_3P$	35.6	*m/z* 233 - $C_9H_{17}O_5N_2$	C_{17}	DAG $C_{32:0}$	2.3
									60.0
	1077.805	1077.805	−0.3	$C_{58}H_{114}O_{13}N_2P$	34.6	Glucosamine	C_{15}	AEG $C_{31:1}$	0.5
	1078.790	1078.789	1.0	$C_{58}H_{113}O_{14}NP$	26.6	Hexose	C_{16}	AEG $C_{30:1}$	1.9
	1078.789	1078.789	0.0	$C_{58}H_{113}O_{14}NP$	28.1	Hexose	C_{16}	AEG $C_{30:1}$	1.4
	1079.785	1079.785	0.0	$C_{57}H_{112}O_{14}N_2P$	30.5	Glucosamine	C_{15}	DAG $C_{30:0}$	1.6
	1080.769	1080.769	0.0	$C_{57}H_{111}O_{15}NP$	24.7	Hexose	C_{15}	DAG $C_{30:0}$	1.7
	1091.784	1091.785	−0.3	$C_{58}H_{112}O_{14}N_2P$	34.4	Glucosamine	C_{31} *iso*DA	lyso-C_{15}	0.4
	1091.820	1091.821	−1.0	$C_{59}H_{116}O_{13}N_2P$	35.3	Glucosamine	C_{15}	AEG $C_{32:1}$	1.3
	1092.806	1092.805	1.0	$C_{59}H1_{15}O_{14}NP$	34.5	Hexose	C_{17}	AEG $C_{30:1}$	1.9
	1093.800	1093.800	0.0	$C_{58}H_{114}O_{14}N_2P$	32.7	Glucosamine	$C_{15/16}$	DAG $C_{30:0}/C_{32:0}$	3.4
	1094.784	1094.784	0.0	$C_{58}H_{113}O_{15}NP$	25.1	Hexose	$C_{15/16}$	DAG $C_{30:0}/C_{32:0}$	0.7
	1094.784	1094.784	0.0	$C_{58}H_{113}O_{15}NP$	26.6	Hexose	$C_{15/16}$	DAG $C_{30:0}/C_{32:0}$	1.6
	1105.800[c]	1105.800	0.0	$C_{59}H_{114}O_{14}N_2P$	35.0	Glucosamine	C_{32} *iso*DA	lyso-C15	0.8
	1107.816	1107.815	1.0	$C_{59}H_{116}O_{14}N_2P$	33.5	Glucosamine	$C_{15/17}$	DAG $C_{30:0}/C_{32:0}$	4.5
	1107.815	1107.816	−1.0	$C_{59}H_{116}O_{14}N_2P$	35.0	Glucosamine	C_{16}	DAG $C_{31:0}$	1.1
	1108.800	1108.800	0.0	$C_{59}H1_{15}O_{15}NP$	27.2	Hexose	$C_{15/17}$	DAG $C_{30:0}/C_{32:0}$	4.0
	1108.799	1108.800	−1.0	$C_{59}H1_{15}O_{15}NP$	28.3	Hexose	$C_{15/17}$	DAG $C_{30:0}/C_{32:0}$	0.8
	1119.816	1119.816	0.2	$C_{59}H_{112}O_{15}N_2P$	26.4	Glucosamine	C_{30} isoDA	lyso-C16	0.1
	1121.832	1121.832	0.0	$C_{60}H_{118}O_{14}N_2P$	33.9	Glucosamine	C_{17}	DAG $C_{31:0}$	0.5
	1121.832	1121.832	0.0	$C_{60}H_{118}O_{14}N_2P$	35.6	Glucosamine	C_{16}	DAG $C_{32:0}$	4.7
	1122.816	1122.816	0.0	$C_{60}H_{117}O_{15}NP$	27.6	Hexose	$C_{17/15}$	DAG $C_{31:0}/C_{33:0}$	1.1
	1122.815	1122.816	−1.0	$C_{60}H_{117}O_{15}NP$	28.9	Hexose	$C_{15/16}$	DAG $C_{31:0}/C_{32:0}$	1.8
	1135.811	1135.811	0.0	$C_{60}H_{116}O_{15}N_2P$	26.7	*N*-acetylglucosamine	C_{16}	DAG $C_{30:0}$	0.9
	1135.847[d]	1135.847	0.0	$C_{61}H_{120}O_{14}N_2P$	36.4	Glucosamine	C_{17}	DAG $C_{32:0}$	5.0
	1136.831	1136.831	0.0	$C_{61}H_{119}O_{15}NP$	29.8	Hexose	C_{17}	DAG $C_{32:0}$	3.3
	1149.826	1149.826	0.0	$C_{61}H_{118}O_{15}N_2P$	27.4	*N*-acetylglucosamine	$C_{15/17}$	DAG $C_{30:0}$/ $C_{32:0}$	1.9
	1162.821	1162.822	−1.0	$C_{61}H_{117}O_{15}N_3P$	30.0	*m/z* 247 - $C_{10}H_{19}O_5N_2$	C_{30} *iso*DA	lyso-C15	0.3
	1163.842	1163.842	0.0	$C_{62}H_{120}O_{15}N_2P$	29.5	*N*-acetylglucosamine	$C_{15/16}$	DAG $C_{31:0}/C_{32:0}$	1.2
	1164.837	1164.837	0.0	$C_{61}H_{119}O_{15}N_3P$	29.1	*m/z* 247 - $C_{10}H_{19}O_5N_2$	C_{15}	DAG $C_{30:0}$	4.5
	1177.857	1177.858	−1.0	$C_{63}H_{122}O_{15}N_2P$	30.2	*N*-acetylglucosamine	C_{17}	DAG $C_{32:0}$	1.6
	1178.853[e]	1178.853	0.0	$C_{62}H_{121}O_{15}N3P$	29.6	*m/z* 247 - $C_{10}H_{19}O_5N_2$	C_{15}	DAG $C_{31:0}$	1.0
	1178.852	1178.853	−1.0	$C_{62}H_{121}O_{15}N_3P$	31.3	*m/z* 247 - $C_{10}H_{19}O_5N_2$	C_{16}	DAG $C_{30:0}$	3.5
	1192.869	1192.869	0.0	$C_{63}H_{123}O_{15}N_3P$	32.0	*m/z* 247 - $C_{10}H_{19}O_5N_2$	$C_{15/17}$	DAG $C_{30:0}/C_{32:0}$	7.9
	1192.866	1192.869	−3.0	$C_{63}H_{123}O_{15}N3P$	33.4	*m/z* 247 - $C_{10}H_{19}O_5N_2$	C_{16}	DAG $C_{31:0}$	1.0
	1206.883	1206.884	−1.0	$C_{64}H_{125}O_{15}N_3P$	32.5	*m/z* 247 - $C_{10}H_{19}O_5N_2$	$C_{15/17}$	DAG $C_{31:0}/C_{33:0}$	1.6
	1206.884	1206.884	0.0	$C_{64}H_{125}O_{15}N_3P$	34.2	*m/z* 247 - $C_{10}H_{19}O_5N_2$	$C_{15/16}$	DAG $C_{31:0}/C_{32:0}$	4.3
	1220.900	1220.900	0.0	$C_{65}H_{127}O_{15}N_3P$	34.8	*m/z* 247 - $C_{10}H_{19}O_5N_2$	C_{17}	DAG $C_{32:0}$	5.9
M. thermoacetica									**80.8**
	1077.804	1077.805	−1.0	$C_{58}H_{114}O_{13}N_2P$	34.7	Glucosamine	C_{15}	AEG $C_{31:1}$	1
	1091.820	1091.821	−1.0	$C_{59}H_{116}O_{13}N_2P$	35.29	Glucosamine	C_{15}	AEG $C_{32:1}$	0.7
	1091.821	1091.821	0.0	$C_{59}H_{116}O_{13}N_2P$	36.9	Glucosamine	C_{16}	AEG $C_{31:1}$	0.9
	1105.837	1105.837	0.0	$C_{60}H_{118}O_{13}N_2P$	37.62	Glucosamine	C_{16}	AEG $C_{32:1}$	1.4
	1107.815	1107.816	−1.0	$C_{59}H_{116}O_{14}N_2P$	34.98	Glucosamine	C_{16}	DAG $C_{31:0}$	1.4
	1119.816	1119.816	0.0	$C_{60}H_{116}O_{14}N_2P$	26.76	*N*-acetylglucosamine	C_{15}	AEG $C_{31:1}$	5.3
	1119.816	1119.816	0.0	$C_{60}H_{116}O_{14}N_2P$	28.19	*N*-acetylglucosamine	C_{16}	AEG $C_{30:1}$	1.0
	1121.795	1121.795	0.0	$C_{59}H_{114}O_{15}N_2P$	24.92	*N*-acetylglucosamine	C_{15}	DAG $C_{30:0}$	1.6
	1121.794	1121.795	−1.0	$C_{59}H_{114}O_{15}N_2P$	25.89	*N*-acetylglucosamine	C_{16}	DAG $C_{29:0}$	2.0
	1121.832	1121.832	0.0	$C_{60}H_{118}O_{14}N_2P$	35.61	Glucosamine	$C_{15/16}$	DAG $C_{31:0}/C_{32:0}$	1.1
	1133.831	1133.832	−1.0	$C_{61}H_{118}O_{14}N_2P$	28.89	*N*-acetylglucosamine	C_{15}	AEG $C_{32:1}$	3.1
	1133.832	1133.831	1.0	$C_{61}H_{118}O_{14}N_2P$	28.79	*N*-acetylglucosamine	C_{17}	AEG $C_{30:1}$	1.4
	1133.831	1133.831	0.0	$C_{61}H_{118}O_{14}N_2P$	30.01	*N*-acetylglucosamine	C_{16}	AEG $C_{31:1}$	5.3
	1135.809	1135.811	−2.0	$C_{60}H_{116}O_{15}N_2P$	26.66	*N*-acetylglucosamine	$C_{15/16}$	DAG $C_{30:0}$/ $C_{32:0}$	5.4
	1135.848	1135.847	1.0	$C_{61}H_{120}O_{14}N_2P$	36.36	Glucosamine	C_{17}	DAG $C_{32:0}$	0.6
	1147.847	1147.847	0.0	$C_{62}H_{120}O_{14}N_2P$	30.89	*N*-acetylglucosamine	C_{16}	AEG $C_{32:1}$	1.3
	1149.826	1149.826	0.0	$C_{61}H_{118}O_{15}N_2P$	27.4	*N*-acetylglucosamine	$C_{15/17}$	DAG $C_{31:0}/C_{32:0}$	2.8
	1149.826	1149.826	0.0	$C_{61}H_{118}O_{15}N_2P$	28.53	*N*-acetylglucosamine	C_{16}	DAG $C_{31:0}$	3.6
	1163.842	1163.842	0.0	$C_{62}H_{120}O_{15}N_2P$	29.48	*N*-acetylglucosamine	$C_{15/16}$	DAG $C_{31:0}/C_{32:0}$	4.9
	1177.857	1177.858	−1.0	$C_{63}H_{122}O_{15}N_2P$	30.2	*N*-acetylglucosamine	C_{17}	DAG $C_{32:0}$	2.7
T. oceani									**47.5**
F. ferrireducens	1093.800	1093.800	0.0	$C_{58}H_{114}N_2O_{14}P$	32.8	Glucosamine	C_{16}	DAG $C_{30:0}$	0.8
	1105.800	1105.800	0.0	$C_{59}H_{114}O_{14}N_2P$	26.4	*N*-acetylglucosamine	C_{15}	AEG $C_{30:1}$	1.4

(*continued on next page*)

Table 2 (*continued*)

	Mass (obs)	Mass (calc)	Δmmu	AEC	RT (min)	Sugar	Alkylamine†	Core	%BPC
	1105.800	1105.800	0.0	$C_{59}H_{114}O_{14}N_2P$	27	*N*-acetylglucosamine	C_{15}	AEG $C_{30:1}$	1.5
	1107.816	1107.816	0.0	$C_{59}H_{116}O_{14}N_2P$	35	Glucosamine	C_{16}	DAG $C_{31:0}$	1.0
	1119.816	1119.816	0.0	$C_{60}H_{116}O_{14}N_2P$	28.2	*N*-acetylglucosamine	C_{16}	AEG $C_{30:1}$	5.8
	1121.795	1121.795	0.0	$C_{59}H_{114}O_{15}N_2P$	24.9	*N*-acetylglucosamine	C_{15}	DAG $C_{30:0}$	4.5
	1121.795	1121.795	0.0	$C_{59}H_{114}O_{15}N_2P$	25.9	*N*-acetylglucosamine	C_{16}	DAG $C_{29:0}$	1.2
	1121.832	1121.832	0.0	$C_{60}H_{118}O_{14}N_2P$	35.6	Glucosamine	C_{17}	DAG $C_{31:0}$	0.6
	1133.832	1133.832	0.0	$C_{61}H_{118}O_{14}N_2P$	28.9	*N*-acetylglucosamine	C_{15}	AEG $C_{32:1}$	3.2
	1133.832	1133.832	0.0	$C_{61}H_{118}O_{14}N_2P$	28.8	*N*-acetylglucosamine	C_{17}	AEG $C_{30:1}$	3.2
	1133.832	1133.832	0.0	$C_{61}H_{118}O_{14}N_2P$	30	*N*-acetylglucosamine	C_{16}	AEG $C_{31:1}$	2.8
	1135.811	1135.811	0.0	$C_{60}H_{116}O_{15}N_2P$	26.7	*N*-acetylglucosamine	$C_{15}/_{16}$	DAG $C_{30:0}$/ $C_{32:0}$	7.3
	1149.826	1149.826	0.0	$C_{61}H_{118}O_{15}N_2P$	27.4	*N*-acetylglucosamine	$C_{15}/_{17}$	DAG $C_{30:0}$/ $C_{32:0}$	12.0
	1161.862	1161.863	−1.0	$C_{63}H_{122}O_{14}N_2P$	31.8	*N*-acetylglucosamine	C_{17}	AEG $C_{32:1}$	3.8
	1161.862	1161.863	−1.0	$C_{63}H_{122}O_{14}N_2P$	32.7	*N*-acetylglucosamine	C_{17}	AEG $C_{32:1}$	2.3
	1161.862	1161.863	−1.0	$C_{63}H_{122}O_{14}N_2P$	33.3	*N*-acetylglucosamine	C_{16}	AEG $C_{33:1}$	1.0
	1163.842	1163.842	0.0	$C_{62}H_{120}O_{15}N_2P$	29.5	*N*-acetylglucosamine	$C_{15}/_{16}$	DAG $C_{30:0}$/ $C_{32:0}$	7.7
	1177.858	1177.858	0.0	$C_{63}H_{122}O_{15}N_2P$	30.2	*N*-acetylglucosamine	C_{17}	DAG $C_{32:0}$	8.8
									68.8
	1074.758	1074.757	1.0	$C_{58}H_{109}O_{14}NP$	24.4	Hexose	C_{14}	AEG $C_{32:3}$	3.4
	1076.774	1076.773	1.0	$C_{58}H_{111}O_{14}NP$	26.8	Hexose	C_{14}	AEG $C_{32:3}$	3.2
	1090.753	1090.752	1.0	$C_{58}H_{109}O_{15}NP$	23.0	Hexose	$C_{14}/_{16}$	DAG $C_{32:2}$ /$C_{30:2}$	4.3
	1092.769	1092.767	2.0	$C_{58}H_{111}O_{15}NP$	25.1	Hexose	$C_{14}/_{16}$	DAG $C_{32:1}$ /$C_{30:1}$	4.0
	1102.789	1102.788	1.0	$C_{60}H_{113}O_{14}NP$	26.9	Hexose	C_{16}	AEG $C_{32:3}$	7.4
	1104.805	1104.805	0.0	$C_{60}H_{115}O_{14}NP$	29.6	Hexose	C_{16}	AEG $C_{32:2}$	6.2
	1100.774	1100.772	2.0	$C_{60}H_{111}O_{14}NP$	24.6	Hexose	C_{16}	AEG $C_{32:3}$	2.1
	1116.769	1116.767	2.0	$C_{60}H_{111}O_{15}NP$	23.4	Hexose	C_{16}	DAG $C_{32:3}$	3.7
	1118.784	1118.783	1.0	$C_{60}H_{113}O_{15}NP$	25.3	Hexose	C_{16}	DAG $C_{32:2}$	9.1
	1120.800[f]	1120.799	1.0	$C_{60}H_{115}O_{15}NP$	27.8	Hexose	C_{16}	DAG $C_{32:1}$	7.1
	1130.784	1130.783	1.0	$C_{61}H_{113}O_{15}NP$	24.0	Hexose	C_{16}	DAG $C_{32:3}$	1.3
	1132.800	1132.798	2.0	$C_{61}H1_{15}O_{15}NP$	26.2	Hexose	C_{16}	DAG $C_{33:2}$	3.3
	1134.816	1134.814	2.0	$C_{61}H_{117}O_{15}NP$	28.7	Hexose	C16	DAG $C_{33:1}$	2.7
	1144.800	1144.797	3.0	$C_{62}H1_{15}O_{15}NP$	25.5	Hexose	C_{16}	DAG $C_{34:3}$	2.4
	1146.816	1146.813	3.0	$C_{62}H_{117}O_{15}NP$	27.8	Hexose	C16	DAG $C_{34:2}$	5.0
	1148.831	1148.830	1.0	$C_{62}H_{119}O_{15}NP$	30.8	Hexose	C_{16}	DAG $C_{34:1}$	2.5
D. gibsoniae									**67.7**
	1091.820	1091.821	−1.0	$C_{59}H_{116}O_{13}N_2P$	28.6	*N*-acetylglucosamine	C_{17}	1,2 diol & C_{14} fatty acid	2.4
	1105.836	1105.837	−1.0	$C_{60}H_{118}O_{13}N_2P$	30.0	*N*-acetylglucosamine	C_{17}	1,2 diol & C_{15} fatty acid	3.7
	1119.852	1119.852	0.0	$C_{61}H_{120}O_{13}N_2P$	31.3	*N*-acetylglucosamine	C_{17}	1,2 diol & C_{16} fatty acid	3.3
	1133.868[g]	1133.868	0.0	$C_{62}H_{122}O_{13}N_2P$	32.7	*N*-acetylglucosamine	C_{17}	1,2 diol & C_{17} fatty acid	3.9
	1147.883	1147.884	−1.0	$C_{63}H_{124}O_{13}N_2P$	34.1	*N*-acetylglucosamine	C_{17}	1,2 diol & C_{18} fatty acid	1.9
	1163.842	1163.842	0.0	$C_{62}H_{120}O_{15}N_2P$	29.5	*N*-acetylglucosamine	C_{16}	DAG $C_{32:0}$	1.1
	1177.857	1177.858	−1.0	$C_{63}H_{122}O_{15}N_2P$	30.2	*N*-acetylglucosamine	C_{17}	DAG $C_{32:0}$	1.4
	1191.872	1191.873	−1.0	$C_{64}H_{124}O_{15}N_2P$	31.3	*N*-acetylglucosamine	C_{17}	DAG $C_{33:0}$	1.5
S. thermosulfidooxidans									**19.2**
	1051.720	1051.719	1.0	$C_{54}H_{104}O_{15}N_2P$	19.98	*N*-acetylglucosamine	C_{14}	DAG $C_{26:0}$	2.6
	1065.736	1065.734	2.0	$C_{55}H_{106}O_{15}N_2P$	20.9	*N*-acetylglucosamine	C_{14}	DAG $C_{27:0}$	3.2
	1077.735	1077.735	0.0	$C_{56}H_{106}O_{15}N_2P$	20.7	*N*-acetylglucosamine	C_{14}	DAG $C_{28:1}$	7.1
	1079.751	1079.751	0.0	$C_{56}H_{108}O_{15}N_2P$	22.2	*N*-acetylglucosamine	C_{14}	DAG $C_{28:0}$	7.7
	1091.751	1091.751	0.0	$C_{57}H_{108}O_{15}N_2P$	21.4	*N*-acetylglucosamine	C_{14}	DAG $C_{29:1}$	5.3
	1093.767	1093.767	0.0	$C_{57}H_{110}O_{15}N_2P$	23.4	*N*-acetylglucosamine	C_{14}	DAG $C_{29:0}$	5.3
	1105.766	1105.765	1.0	$C_{58}H_{110}O_{15}N_2P$	23.1	*N*-acetylglucosamine	C_{14}	DAG $C_{30:1}$	8.2
	1119.782	1119.779	3.0	$C_{59}H_{112}O_{15}N_2P$	23.9	*N*-acetylglucosamine	C_{14}	DAG $C_{31:1}$	4.9
H. cellulosilytica									**44.3**
	1108.800	1108.800	0.0	$C_{59}H1_{15}O_{15}NP$	32.56	Glucosamine	C_{17} *	DAG $C_{30:0}$	4.0
	1136.831	1136.831	0.0	$C_{61}H_{119}O_{15}NP$	35.36	Glucosamine	C_{17} *	DAG $C_{32:0}$	1.8
	1135.811	1135.810	1.0	$C_{60}H_{116}O_{15}N_2P$	26.9	*N*-acetylglucosamine	C_{17}	DAG $C_{29:0}$	6.4
	1149.827	1149.826	1.0	$C_{61}H_{118}O_{15}N_2P$	27.3	*N*-acetylglucosamine	C_{17}	DAG $C_{30:0}$	22.5
	1151.807	1151.806	1.0	$C_{60}H_{116}O_{16}N_2P$	28.87	*m/z* 233 - $C_9H_{17}O_5N_2$	C_{17} *	DAG $C_{29:0}$	2.5
	1163.842	1163.842	0.0	$C_{62}H_{120}O_{15}N_2P$	29.7	*N*-acetylglucosamine	C_{17}	DAG $C_{31:0}$	2.9
	1165.821	1165.821	0.0	$C_{61}H_{118}O_{16}N_2P$	31.01	*m/z* 233 - $C_9H_{17}O_5N_2$	C_{17} *	DAG $C_{29:0}$	3.7
	1177.860	1177.858	2.0	$C_{63}H_{122}O_{15}N_2P$	20.28	*N*-acetylglucosamine	C_{17}	DAG $C_{32:0}$	10.7
	1179.837[h]	1179.837	0.0	$C_{62}H_{120}O_{16}N_2P$	31.71	*m/z* 233 - $C_9H_{17}O_5N_2$	C_{17} *	DAG $C_{30:0}$	13.1
	1179.836	1179.837	−1.0	$C_{62}H_{120}O_{16}N_2P$	28.81	*N*-acetylglucosamine	C_{17}	DAG $C_{31:0}$ - OH	0.5
	1207.868	1207.868	0.0	$C_{64}H_{124}O_{16}N_2P$	34.82	*m/z* 233 - $C_9H_{17}O_5N_2$	C_{17} *	DAG $C_{32:0}$	4.4
C. subterraneus									**72.6**

All masses represent an $[M+H]^+$ ion. Mass (obs) = Observed mass; Mass (calc) = calculated mass. Δmmu = the difference between the measured mass calculated mass x 1000; AEC = assigned elemental composition; RT = retention time. % BPC = peak area as a percent of the area of the total base peak chromatogram. Core nomenclature, DAG = diacyl glycerol; AEG = acyl/ether glycerol; Cx:y denotes the total of non-glycerol carbon atoms (x) of the glycerol-bound core (cf. Fig. 1) and the number of unsaturations (y). * = not an N-glyceroyl alkylamine but a glyceroylalkyl. †From LCMS analysis it is not possible determine whether the N-glyceroyl alkylamine moieties are straight chain or branched. For examples of mass spectra see: [a]Fig. 7; [b]Fig. S2; [c]Fig. 9; [d]Fig. 6; [e]Fig. S1; [f]Fig. S3; [g]Fig. 8; [h]Fig. S4.

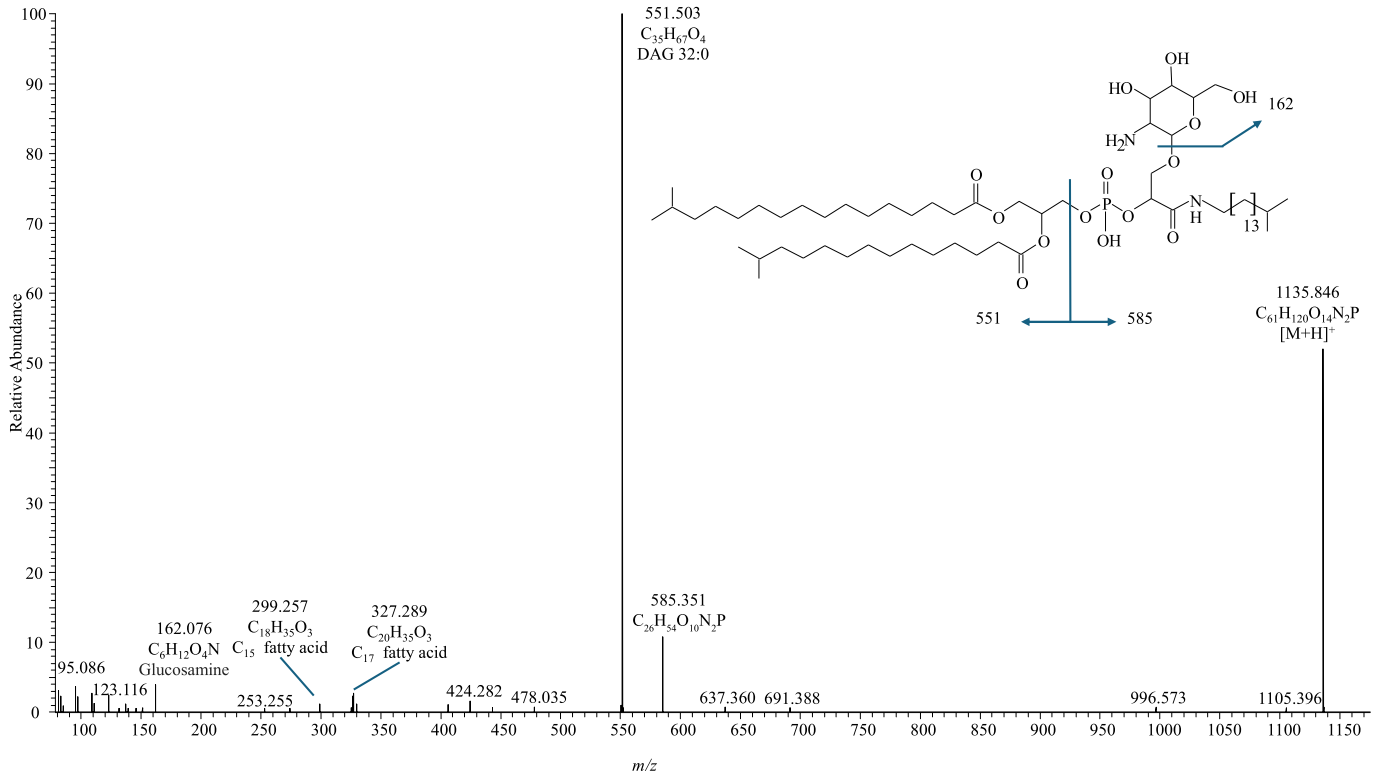

Fig. 6. MS^2 spectrum of a NGAP with *m/z* 1135.847 obtained by UHPLC-HRMS^n analysis of the IPL extract of *M. thermoacetica* (Table 2). The accurate masses and corresponding elemental formula of the $[M + H]^+$ and some abundant fragment ions are indicated. This NGAP has a fully saturated diacyl glycerol (DAG) core with 32 non-glycerol carbon atoms. The sugar is glucosamine, as evident from the fragment ion at *m/z* 162.076. The indicated structure of this compound is tentative.

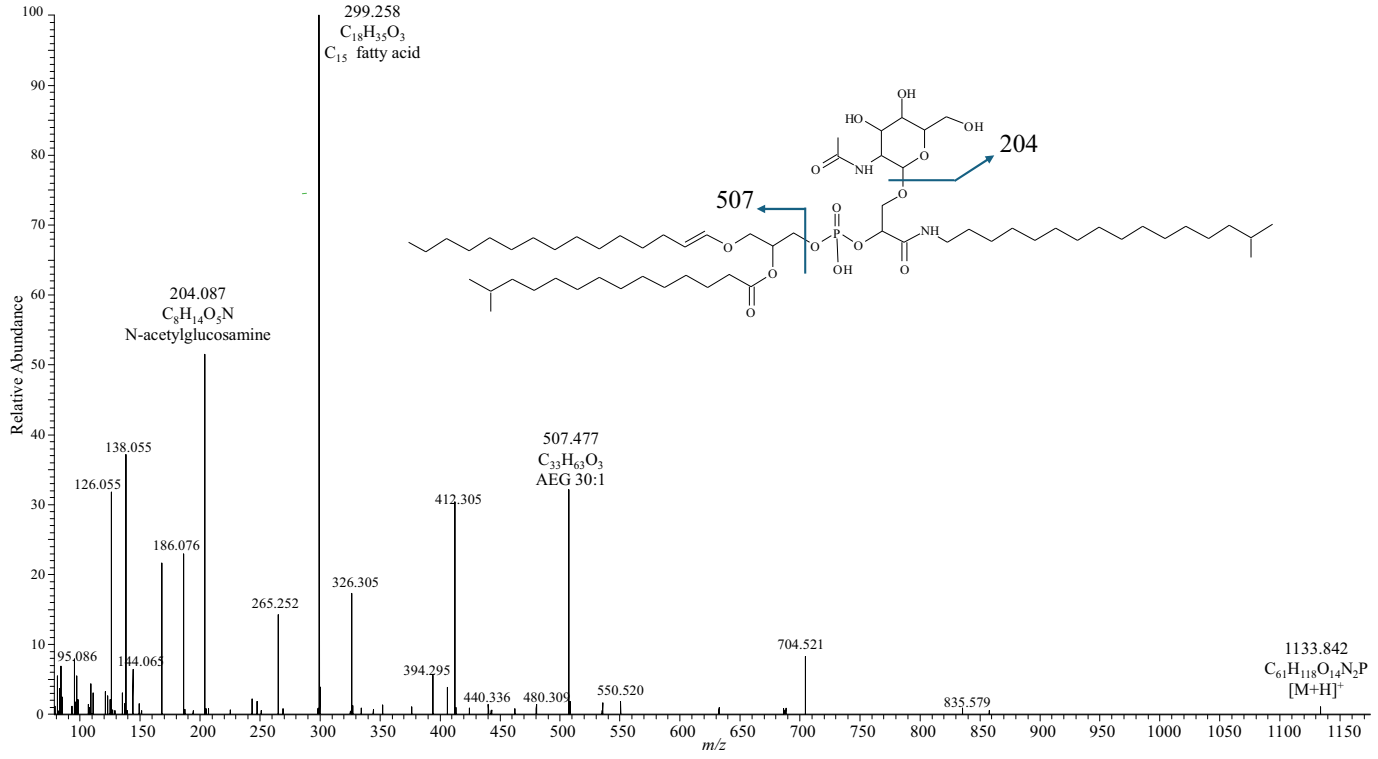

Fig. 7. MS^2 spectrum of a NGAP with *m/z* 1133.832 obtained by UHPLC-HRMS^n analysis of the IPL extract of *T. wiegelii* (Table 2). The accurate masses and corresponding elemental formulae of the $[M + H]^+$ and some abundant fragment ions are indicated. This NGAP has an acyl/ether glycerol (AEG) core with 30 non-glycerol carbons and one unsaturation (position of the double bond is not known but assumed to be as in a plasmalogen). The sugar is an *N*-acetylglucosamine as evident from the fragment ion at *m/z* 204.067. The indicated structure of this compound is tentative.

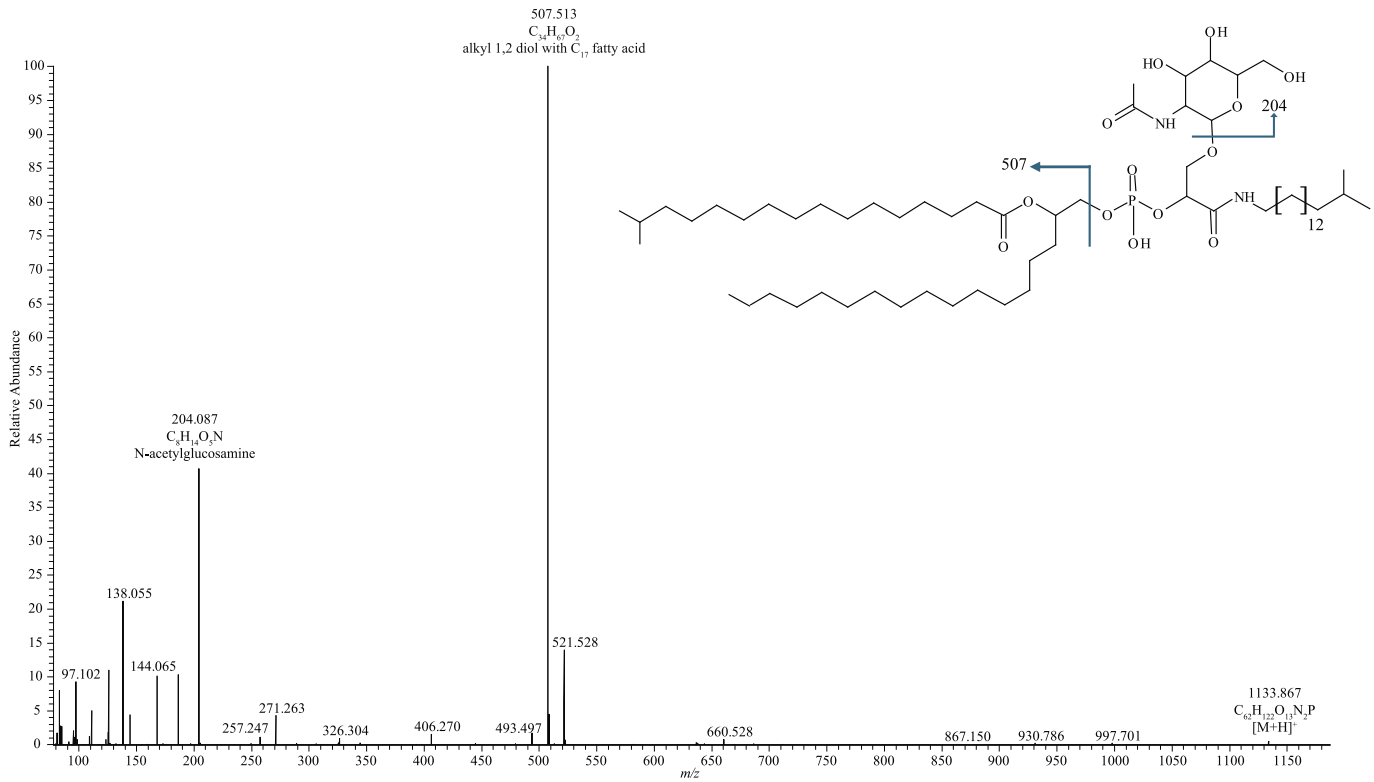

Fig. 8. MS^2 spectrum of NGAP with *m/z* 1133.868 obtained by UHPLC-$HRMS^n$ analysis of the IPL extract of *S. thermosulfidooxidans* (Table 2). The accurate masses and corresponding elemental formula of the $[M + H]^+$ and some abundant fragment ions are indicated. This NGAP is postulated to have an alkyl 1,2-diol with an *iso*-C_{17} fatty acid as its core. The sugar is an *N*-acetylglucosamine as evident from the fragment ion at *m/z* 204.067. The indicated structure of this compound is tentative.

glyceroyl alkylamine phosphoglycolipids with an N-containing sugar with elemental composition of $C_9H_{17}N_2O_5$. Finally, two strains, *D. gibsoniae* and *M. thermoacetica*, contained NGAPs with a hexose sugar.

Overall, the carbon number of the alkylamine moieties, as determined by UHPLC-$HRMS^n$ (Table 2), was the same as that of hydrolysis-derived NGAs, as determined by GC–MS, ranging in length between 14 and 17 carbons. The carbon number and degree of unsaturation of the glycerol-bound core, as determined by UHPLC-$HRMS^n$ (Table 2), was also generally in agreement with the hydrolysis-derived lipid distributions, as determined by GC–MS, for each strain (Table S1). All strains made NGAPs with DAG cores (MS^2 spectrum Fig. 6) and/or AEG cores (MS^2 spectrum Fig. 7) except for *S. thermosulfidooxidans,* which contained NGAPs with DAG and alkyl 1,2-diol fatty acid cores (MS^2 spectrum Fig. 8). As mentioned above, *C. subterraneus* also contained IPLs postulated to contain glyceroylalkyls rather than NGAs (Table 2). NGAPs with long-chain (C_{30} – C_{32}) NGAs were only detected in *M. thermoacetica* biomass, in agreement with GC–MS analysis (Table S1).

Discussion

The *Bacillota* phylum was originally known as *Firmicutes*, a name that is derived from the Latin for “tough skin”. While analyzing the membrane lipids of different *Bacillota*, we found that nine *Bacillota* strains, from two classes (*Clostridia* and *Sulfobacillia*), produce NGAs, lipids that have, to date, only been described in extremophiles from the *Deinococcota* and *Armatimonadota* phyla. Despite their distribution over 5 orders of *Bacillota*, these lipids are not a uniform characteristic of members of the phylum, indeed the 9 other *Bacillota* strains examined were not found to produce these unusual lipids (Table 1). Of the 9 strains that were found to produce NGAs, 7 were thermophilic (Table 1), as their optimum growth temperature exceeded 45 °C (Madigan et al., 2014). The remaining two non-thermophilic strains were *D. gibsoniae* (cultured at 35 °C) and the halophilic *H. cellulosilytica* (cultured at 37 °C). Conversely, of the 9 *Bacillota* strains that did not produce the NGAs, 8 were mesophilic and were cultured between 30 and 40 °C. This suggests that NGA lipids may contribute to membrane stability under thermophilic conditions. The one exception was *C. owensensis*, falling in the *Thermoanaerobacterales*. This strain is thermophilic and was cultured at 70 °C and did not produce NGAs under these conditions. Overall its hydrolysis-derived lipid distribution was quite similar to that of the other four *Thermoanaerobacterales*, all of which did produce NGAs. It is possible that *C. owensensis* is able to produce NGAs but under different growth conditions. Indeed, it should be noted that in this study, all *Bacillota* strains were grown to maximize biomass production for lipid analysis and were hence harvested in the late exponential phase to the beginning stationary phase. Whether the lipid composition of these strains would be the same as those described here under varying conditions, such as a different growth stage or different culturing conditions is currently not known. One other notable difference between *C. owensensis* and the other 4 *Thermoanaerobacterales* species was that its fatty acid distribution is dominated by *iso*-$C_{17:0}$ in contrast to the other four strains where *iso*-$C_{15:0}$ fatty acid was the most abundant (Table S1).

Other strains from outside the *Bacillota* which are known to produce NGA lipids include *Deinococcus radiodurans*, species of the *Thermus* and *Meiothermus* genera and *Chthonomonas calidirosea* (Anderson, 1983; Yang et al., 2006; Compton et al., 2020); all being extremophilic thermophiles. Furthermore, intact polar NGAP lipids have been detected in the lipidome of hot spring streamer biofilms from Yellowstone National Park, where they were surmised to originate from *Thermus* and *Meiothermus* bacteria (Schubotz et al., 2013, 2015; Boyer et al., 2020). Hence it would seem that the presence of NGAs appears to be associated with thermophilia.

The *Bacillota* is an unusual phylum in that it has members with both monoderm and diderm cell envelopes and hence a mix of Gram-positive and Gram-negative cell wall types (Choi et al., 2024). Indeed, the 18 strains examined here have a mix of positive and negative staining

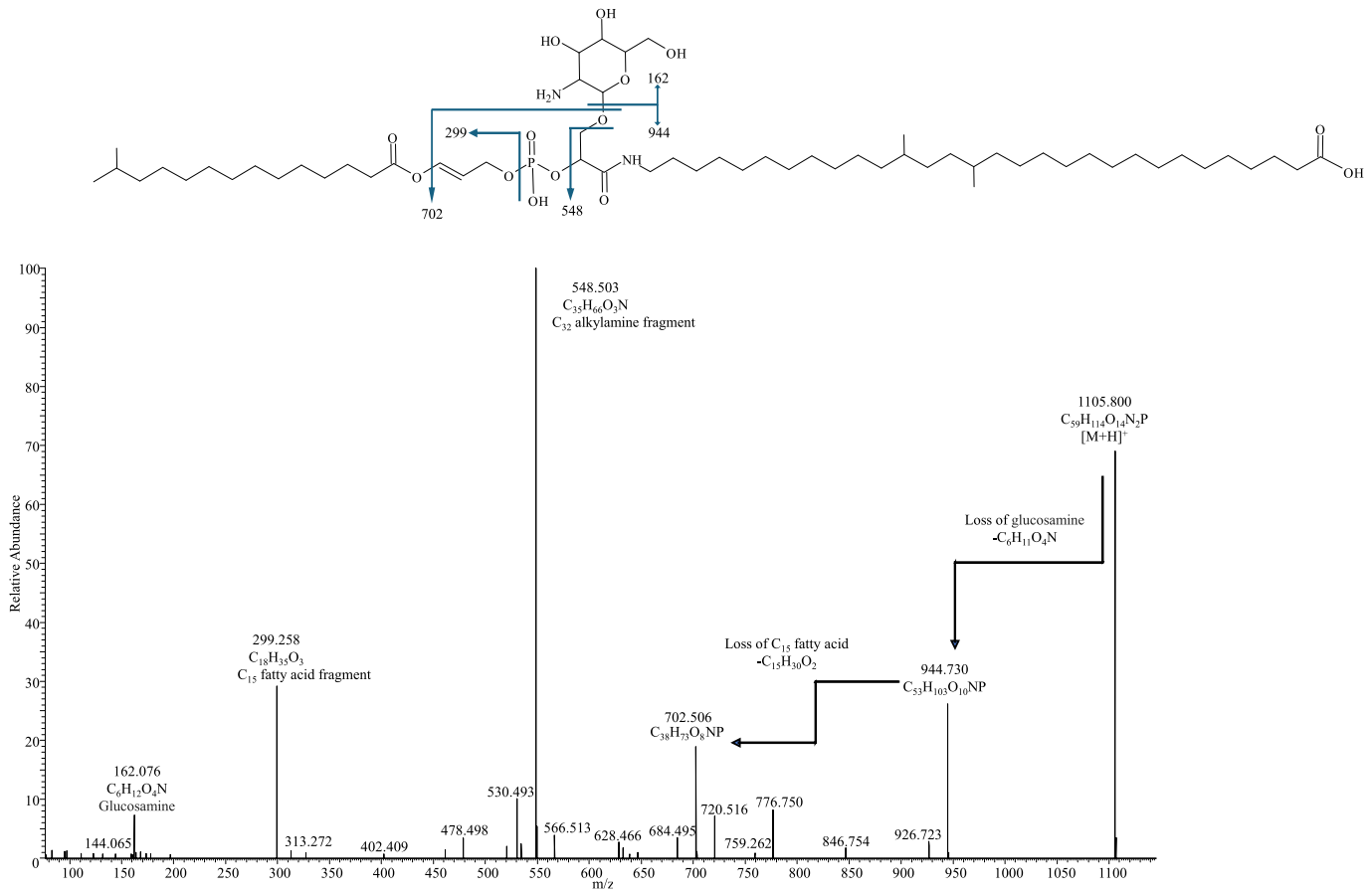

Fig. 9. MS^2 spectrum of a NGAP with *m/z* 1105.800 detected by UHPLC-$HRMS^n$ analysis of the IPL extract of *M. thermoacetica* (Table 2). The accurate masses and corresponding elemental formula of the $[M + H]^+$ and some abundant fragment ions are indicated. The IPL is assumed to have a lyso core with 15 non-glycerol carbons. The sugar is glucosamine, as evident from the fragment ion at *m/z* 162.076. The ion at *m/z* 548.503 is assigned as a C_{32} alkylamine, as was also detected by GC–MS analysis (Fig. 4). The indicated structure of this compound is tentative.

membranes, even within the same orders (Table 1). However, there does not appear to be a clear correlation between the presence or absence of NGAs in relation to Gram-positive or Gram-negative staining. However, this may explain in part the variability in the lipid composition between the 18 *Bacillota* strains examined, even within orders.

Eight of the strains found to produce NGA lipids were examined for their intact polar lipid composition (Table 2). A wide range of different NGAPs were detected, ranging in the composition of their sugar moiety, acyl or alkyl 1,2-diol core and alkylamine length. All strains were found to produce NGAPs with nitrogen sugars, except for *D. gibsoniae* which only produced hexose sugar moieties (Table 2). This strain is the only mesophilic strain of the group, neither thermophilic nor halophilic (Table 1). Six strains produced mostly NGAPs with *N*-acetylglucosamine sugars. Conversely one strain, *M. thermoacetica*, had a much more diverse range of sugars moieties in its NGAPs: 7 % *N*-acetylglucosamine, 26 % hexose, 29 % glucosamine sugar and 38 % an N sugar postulated to have a formula $C_{10}H_{20}O_6N_2$ (cf. Fig. S1).

The majority of the NGAPs comprise a DAG core, with the second most common core an AEG core, and only one strain producing 1,2-diols cores. A number of bacteria are known to synthesize ether containing lipids, including plasmalogens, saturated, mixed ether/ester and diether lipids (Hamilton-Brehm et al., 2013; Grossi et al., 2015; Krake et al., 2022; Sinninghe Damsté et al., 2023; Ding et al., 2024). It is thought that the presence of ether lipids in bacterial membranes aids adaptation to extreme conditions such as high temperature (Sahonero-Canavesi et al., 2022b) or low pH (Sánchez-Andrea et al., 2022). However, it should also be noted that mesophilic bacteria also do produce ether lipids (e.g. Rütters et al., 2001; Ding et al., 2024). A series of compounds, postulated to be phosphoglycolipids with glyceroylalkyls rather than NGAs, were detected in *C. subterraneus* (Table 2; see Fig. S4 for example MS^2 spectrum). It is interesting to note that this strain also produced wax esters (Table S1, Fig. 2a), which accounted for up to ~1.2 % of the hydrolysis-derived lipids detected, but which we do not expect are hydrolysis products of the glyceroylalkyl phosphoglycolipids.

Alkyl 1,2-diols have been detected previously in green-non sulfur bacteria such as *Thermomicrobium roseum* (Pond et al., 1986) and in the class *Thermomicrobia* class (Lagutin et al., 2015), where they are known to act as core lipids for their membranes. In our study we found that the acid-hydrolysate of *S. thermosulfidooxidans* also contained alkyl 1,2-diols and we were able to link these to intact polar NGAs, which we assigned as having an alkyl 1,2-diol bound to a fatty acid as their core (Fig. 8), in place of the more-common diacyl glycerol core (cf. Fig. 6). Similar NGAs have previously been detected in the thermophilic bacteria *M. ruber* (Yang et al., 2006; Lin et al., 2013; Lagutin et al., 2014).

Hydrolysis-derived lipid analysis revealed that *M. thermoacetica* contained long-chain (C_{30}-C_{32}) N-glyceroyl alkylamines with carboxylic acids at the end of the chains (Fig. 5), a characteristic not seen in the other strains (Table S1). These long-chain NGAs were similar in structure to the membrane spanning lipids found in the *Thermoanaerobacterales* and *Thermosediminibacterales* orders (Table S1) such as isodiabolic acid. NGAPs were also found that contained the long-chain NGAs (Fig. 9, Table 2). It is not possible from our analysis to know whether the long-chain NGA moiety acts as a polar headgroup, outside the lipid bilayer (as drawn in Fig. 9), or whether the entire lipid is in a different configuration that allows the long-chain NGAs to act as membrane spanning lipids. Membrane-spanning lipids are common in

archaea, in the form of isoprenoidal glycerol dialkyl glycerol tetraethers, where they improve the rigidity and impermeability of the membrane, relative to a lipid bilayer (Schouten et al., 2013). Conversely membrane spanning lipids are rare in bacteria (Sahonero-Canavesi et al., 2022a), but are present in *M. thermoacetica* (Table S1).

Conclusions

We found that nine strains of *Bacillota*, produce unusual NGA lipids. A further nine *Bacillota* strains were not found to produce these lipids. One strain, *M. thermoacetica* was found to produce long-chain NGAs (C_{30}-C_{32}). Across the NGA producing strains, a wide range of intact polar NGAPs were detected, ranging in the composition of their sugar moiety, core and alkylamine. The presence of NGAs appears to be associated with thermophilia.

CRediT authorship contribution statement

Nicole J. Bale: Writing – review & editing, Writing – original draft, Visualization, Supervision, Project administration, Investigation, Formal analysis. **Michel Koenen:** Writing – review & editing, Investigation. **Su Ding:** Writing – review & editing, Investigation. **Jaap S. Sinninghe Damsté:** Writing – review & editing, Writing – original draft, Visualization, Supervision, Project administration, Investigation, Funding acquisition, Formal analysis, Conceptualization.

Funding

This study was supported by the European Research Council (ERC) under the European Union's Horizon 2020 research and innovation program (grant agreement no. 694569-MICROLIPIDS to JSSD) and by the Soehngen Institute for Anaerobic Microbiology (SIAM) through a Dutch Gravitation Grant (grant no. 024.002.002 to JSSD).

Declaration of competing interest

The authors declare that they have no known competing financial interests or personal relationships that could have appeared to influence the work reported in this paper.

Acknowledgments

We thank Dr. Meina Neumann-Schaal and colleagues at DSMZ-Deutsche Sammlung von Mikroorganismen und Zellkulturen for growth and harvesting of the biomass used in this study. We thank Dr. Diana Sahonero Canavesi for providing the *T. ethanolicus* lipid extracts and for helpful discussions. We also thank Prof. Stefan Schouten and Dr. Marcel van der Meer for help with chemical nomenclature. Denise Dorhout and Monique Verweij are acknowledged for their technical support. We also thank two reviewers for their helpful and constructive suggestions and edits.

Appendix A. Supplementary data

Supplementary data to this article can be found online at https://doi.org/10.1016/j.syapm.2025.126609.

Data availability

All data is available in the published manuscript or stored in public databases.

References

Anderson, R., 1983. Alkylamines: novel lipid constituents in *Deinococcus radiodurans*. Biochemica et Biophysica Acta 753, 266–268.

Anderson, R., Hansen, K., 1985. Structure of a novel phosphoglycolipid from *Deinococcus radiodurans*. J. Biol. Chem. 260, 12219–12223.

Balch, W.M., Schoberth, S., Tanner, R.S., Wolfe, R.S., 1977. Acetobacterium, a new genus of hydrogen-oxidizing, carbon dioxide-reducing, anaerobic Bacteria. Int. J. Syst. Evol. Microbiol. 27, 355–361.

Bale, N.J., Rijpstra, W.I.C., Oshkin, I.Y., Belova, S.E., Dedysh, S.N., Sinninghe Damsté, J. S., 2019. Fatty acid and hopanoid adaption to cold in the methanotroph *Methylovulum psychrotolerans*. Front. Microbiol. 10, 589.

Bale, N.J., Ding, S., Hopmans, E.C., Arts, M.G.I., Villanueva, L., Boschman, C., Haas, A.F., Schouten, S., Sinninghe Damsté, J.S., 2021. Lipidomics of environmental microbial communities. I: visualization of component distributions using untargeted analysis of high-resolution mass spectrometry data. Front. Microbiol. 12.

Bosak, T., Schubotz, F., de Santiago-Torio, A., Kuehl, J.V., Carlson, H.K., Watson, N., Daye, M., Summons, R.E., Arkin, A.P., Deutschbauer, A.M., 2016. System-wide adaptations of *Desulfovibrio alaskensis* G20 to phosphate-limited conditions. PLoS One 11, e0168719.

Boyer, G.M., Schubotz, F., Summons, R.E., Woods, J., Shock, E.L., 2020. Carbon oxidation state in microbial polar lipids suggests adaptation to hot spring temperature and redox gradients. Front. Microbiol. 11. https://doi.org/10.3389/fmicb.2020.00229.

Campbell, L.L., Postgate, J.R., 1965. Classification of the spore-forming sulfate-reducing bacteria. Bacteriol. Rev. 29, 359–363.

Cayol, J.L., Ollivier, B., Patel, B.K., Ageron, E., Grimont, P.A., Prensier, G., Garcia, J.L., 1995. Haloanaerobium lacusroseus sp. nov., an extremely halophilic fermentative bacterium from the sediments of a hypersaline lake. Int. J. Syst. Bacteriol. 45, 790–797.

Choi, J.K., Poudel, S., Yee, N., Goff, J.L., 2024. Deeply branching Bacillota species exhibit atypical gram-negative staining. Microbiology Spectrum 12, e00732–e00824.

Clarke, N.G., Hazlewood, G.P., Dawson, R.M., 1980. Structure of diabolic acid-containing phospholipids isolated from *Butyrivibrio* sp. Biochem. J. 191, 561–569.

Compton, B.J., Lagutin, K., Dyer, B.S., Ryan, J., MacKenzie, A., Stott, M.B., Nekrasov, E. V., Painter, G.F., Vyssotski, M., 2020. Isolation and synthesis of Glycophospholipids from the extremophile *Chthonomonas calidirosea*. Asian J. Org. Chem. 9, 1802–1814.

Cook, G.M., Rainey, F.A., Patel, B.K.C., Morgan, H.W., 1996. Characterization of a new Obligately anaerobic thermophile, Thermoanaerobacter wiegelii sp. nov. Int. J. Syst. Evol. Microbiol. 46, 123–127.

Cox, M.M., Battista, J.R., 2005. *Deinococcus radiodurans* — the consummate survivor. Nat. Rev. Microbiol. 3, 882–892.

Ding, S., Grossi, V., Hopmans, E.C., Bale, N.J., Cravo-Laureau, C., Sinninghe Damsté, J.S., 2024. Nitrogen and sulfur for phosphorus: Lipidome adaptation of anaerobic sulfate-reducing bacteria in phosphorus-deprived conditions. Proc. Natl. Acad. Sci. 121, e2400711121.

Fardeau, M.-L., Salinas, M.B., L'Haridon, S., Jeanthon, C., Verhé, F., Cayol, J.-L., Patel, B. K.C., Garcia, J.-L., Ollivier, B., 2004. Isolation from oil reservoirs of novel thermophilic anaerobes phylogenetically related to Thermoanaerobacter subterraneus: reassignment of T. Subterraneus, Thermoanaerobacter yonseiensis, Thermoanaerobacter tengcongensis and Carboxydibrachium pacificum to Caldanaerobacter subterraneus gen. Nov., sp. nov., comb. nov. as four novel subspecies. Int. J. Syst. Evol. Microbiol. 54, 467–474.

Filippidou, S., Wunderlin, T., Junier, T., Jeanneret, N., Dorador, C., Molina, V., Johnson, D.R., Junier, P., 2016. A combination of extreme environmental conditions favor the prevalence of endospore-forming Firmicutes. Front. Microbiol. 7. https://doi.org/10.3389/fmicb.2016.01707.

Fujimoto, Y., Mitsunobe, K., Fujiwara, S., Mori, M., Hashimoto, M., Suda, Y., Kusumoto, S., Fukase, K., 2013. Synthesis and biological activity of phosphoglycolipids from *Thermus thermophilus*. Org. Biomol. Chem. 11, 5034–5041.

Gan, C.H., Wijaya, H., Li, L.-H., Wei, C.-F., Peng, Y.-J., Wu, S.-H., Hua, K.-F., Lam, Y., 2020. H-phosphonate synthesis and biological evaluation of an immunomodulatory Phosphoglycolipid from thermophilic Bacteria. Org. Lett. 22, 2569–2573.

Geiger, O., Röhrs, V., Weissenmayer, B., Finan, T.M., Thomas-Oates, J.E., 1999. The regulator gene *phoB* mediates phosphate stress-controlled synthesis of the membrane lipid diacylglyceryl-N,N,N-trimethylhomoserine in *Rhizobium (Sinorhizobium) meliloti*. Mol. Microbiol. 32, 63–73.

Geiger, O., González-Silva, N., López-Lara, I.M., Sohlenkamp, C., 2010. Amino acid-containing membrane lipids in bacteria. Prog. Lipid Res. 49, 46–60.

Goldfine, H., 2022. Plasmalogens in bacteria, sixty years on. Front. Mol. Biosci. 9, 962757.

Golovacheva, R.S., Karavaĭko, G.I., 1978. Sulfobacillus, a new genus of thermophilic sporulating bacteria. Mikrobiologiia 47, 815–822.

Grossi, V., Mollex, D., Vinçon-Laugier, A., Hakil, F., Pacton, M., Cravo-Laureau, C., 2015. Mono- and Dialkyl glycerol ether lipids in anaerobic Bacteria: biosynthetic insights from the mesophilic sulfate reducer *Desulfatibacillum alkenivorans* PF2803T. Appl. Environ. Microbiol. 81, 3157–3168.

Hamilton-Brehm, S.D., Gibson, R.A., Green, S.J., Hopmans, E.C., Schouten, S., van der Meer, M.T.J., Shields, J.P., Sinninghe Damsté, J.S., Elkins, J.G., 2013. *Thermodesulfobacterium geofontis* sp nov., a hyperthermophilic, sulfate-reducing bacterium isolated from obsidian Pool. Yellowstone National Park. Extremophiles 17, 251–263.

Huang, Y., Anderson, R., 1989. Structure of a novel glucosamine-containing phosphoglycolipid from *Deinococcus radiodurans*. J. Biol. Chem. 264, 18667–18672.

Huang, C.Y., Patel, B.K., Mah, R.A., Baresi, L., 1998. Caldicellulosiruptor owensensis sp. nov., an anaerobic, extremely thermophilic, xylanolytic bacterium. Int. J. Syst. Bacteriol. 48 Pt 1, 91–97.

Iino, T., Mori, K., Tanaka, K., Suzuki, K.-I., Harayama, S., 2007. Oscillibacter valericigenes gen. Nov., sp. nov., a valerate-producing anaerobic bacterium isolated

from the alimentary canal of a Japanese corbicula clam. Int. J. Syst. Evol. Microbiol. 57, 1840–1845.
Jung, S., Zeikus, J.G., Hollingsworth, R.I., 1994. A new family of very long chain alpha, omega-dicarboxylic acids is a major structural fatty acyl component of the membrane lipids of *Thermoanaerobacter ethanolicus* 39E. J. Lipid Res. 35, 1057–1065.
Krake, N., Birgel, D., Smrzka, D., Zwicker, J., Huang, H., Feng, D., Bohrmann, G., Peckmann, J., 2022. Molecular and isotopic signatures of oil-driven bacterial sulfate reduction at seeps in the southern Gulf of Mexico. Chem. Geol. 595, 120797.
Kuever, J., Rainey, F.A., Hippe, H., 1999. Description of Desulfotomaculum sp. Groll as Desulfotomaculum gibsoniae sp. nov. Int. J. Syst. Bacteriol. 49 Pt 4, 1801–1808.
Lagutin, K., MacKenzie, A., Houghton, K.M., Stott, M.B., Vyssotski, M., 2014. The identification and quantification of phospholipids from *Thermus* and *Meiothermus* Bacteria. Lipids 49, 1133–1141.
Lagutin, K., MacKenzie, A., Houghton, K.M., Stott, M.B., Vyssotski, M., 2015. Novel long-chain diol phospholipids from some Bacteria belonging to the class *Thermomicrobia*. Lipids 50, 303–311.
Lee, Y.-J., Wagner, I.D., Brice, M.E., Kevbrin, V.V., Mills, G.L., Romanek, C.S., Wiegel, J., 2005. Thermosediminibacter oceani gen. Nov., sp. nov. and Thermosediminibacter litoriperuensis sp. nov., new anaerobic thermophilic bacteria isolated from Peru margin. Extremophiles: Life Under Extreme Conditions 9, 375–383.
Lin, H.-J., Adak, A.K., Reddy, L.V.R., Wu, S.-H., Lin, C.-C., 2013. Total synthesis of an immunomodulatory Phosphoglycolipid from thermophilic Bacteria. Chemistry – a. Eur. J. Dermatol. 19, 7989–7998.
Madigan, M.T., Martinko, J.M., Bender, K.S., Buckley, D.H., Stahl, D.A., 2014. Brock Biology of Microorganisms, 14th ed (Pearson).
Ogg, C.D., Patel, B.K.C., 2009. Fervidicola ferrireducens gen. Nov., sp. nov., a thermophilic anaerobic bacterium from geothermal waters of the great Artesian Basin, Australia. Int. J. Syst. Evol. Microbiol. 59, 1100–1107.
Pond, J.L., Langworthy, T.A., Holzer, G., 1986. Long-chain diols: a new class of membrane lipids from a thermophilic bacterium. Science 231, 1134–1136.
Rainey, F.A., Zhilina, T.N., Boulygina, E.S., Stackebrandt, E., Tourova, T.P., Zavarzin, G. A., 1995. The taxonomic status of the fermentative halophilic anaerobic bacteria: description of Haloanaerobiales Ord. Nov., Halobacteroidaceae fam. Nov., Orenia gen. Nov. and further taxonomic rearrangements at the genus and species level. Anaerobe 1, 185–199.
Ravot, G., Magot, M., Ollivier, B., Patel, B.K.C., Ageron, E., Grimont, P.A.D., Thomas, P., Garcia, J.-L., 1997. *Haloanaerobium congolense* sp. nov., an anaerobic, moderately halophilic, thiosulfate- and sulfur-reducing bacterium from an African oil field. FEMS Microbiol. Lett. 147, 89–95.
Rütters, H., Sass, H., Cypionka, H., Rullkötter, J., 2001. Monoalkylether phospholipids in the sulfate-reducing bacteria Desulfosarcina variabilis and Desulforhabdus amnigenus. Arch. Microbiol. 176, 435–442.
Sahonero-Canavesi, D.X., Siliakus, M.F., Abdala Asbun, A., Koenen, M., von Meijenfeldt, F.A.B., Boeren, S., Bale, N.J., Engelman, J.C., Fiege, K., Strack van Schijndel, L., Sinninghe Damsté, J.S., Villanueva, L., 2022a. Disentangling the lipid divide: identification of key enzymes for the biosynthesis of membrane-spanning and ether lipids in Bacteria. Science. Advances 8, eabq8652.
Sahonero-Canavesi, D.X., Villanueva, L., Bale, N.J., Bosviel, J., Koenen, M., Hopmans, E. C., Sinninghe Damsté, J.S., 2022b. Changes in the distribution of membrane lipids during growth of *Thermotoga maritima* at different temperatures: indications for the potential mechanism of biosynthesis of ether-bound diabolic acid (membrane-spanning) lipids. Appl. Environ. Microbiol. 88, e0176321.
Sánchez-Andrea, I., van der Graaf, C.M., Hornung, B., Bale, N.J., Jarzembowska, M., Sousa, D.Z., Rijpstra, W.I.C., Sinninghe Damsté, J.S., Stams, A.J.M., 2022. Acetate Degradation at Low pH by the Moderately Acidophilic Sulfate Reducer *Acididesulfobacillus acetoxydans* gen. nov. sp. nov. Frontiers in Microbiology 13.
Schink, B., 1984. Clostridium magnum sp. nov., a non-autotrophic homoacetogenic bacterium. Arch. Microbiol. 137, 250–255.
Schouten, S., Hopmans, E.C., Sinninghe Damsté, J.S., 2013. The organic geochemistry of glycerol dialkyl glycerol tetraether lipids: a review. Org. Geochem. 54, 19–61.
Schubotz, F., 2019. Membrane homeostasis upon nutrient (C, N, P) limitation. In: Geiger, O. (Ed.), Biogenesis of Fatty Acids, Lipids and Membranes, Handbook of Hydrocarbon and Lipid Microbiology. Springer International Publishing, Cham, pp. 823–847.
Schubotz, F., Meyer-Dombard, D.R., Bradley, A.S., Fredricks, H.F., Hinrichs, K.-U., Shock, E.L., Summons, R.E., 2013. Spatial and temporal variability of biomarkers and microbial diversity reveal metabolic and community flexibility in streamer biofilm communities in the lower Geyser Basin, Yellowstone National Park. Geobiology 11, 549–569.
Schubotz, F., Hays, L.E., Meyer-Dombard, D.R., Gillespie, A., Shock, E.L., Summons, R.E., 2015. Stable isotope labeling confirms mixotrophic nature of streamer biofilm communities at alkaline hot springs. Front. Microbiol. 6. https://doi.org/10.3389/fmicb.2015.00042.
Sharon, N., 1957. Polysaccharide containing amino-sugar from *Bacillus subtilis*. Nature 179, 919.
Sharon, N., 2007. Celebrating the golden anniversary of the discovery of bacillosamine, the diamino sugar of a *Bacillus*. Glycobiology 17, 1150–1155.
Siliakus, M.F., van der Oost, J., Kengen, S.W.M., 2017. Adaptations of archaeal and bacterial membranes to variations in temperature, pH and pressure. Extremophiles 21, 651–670.
Simankova, M.V., Chernych, N.A., Osipov, G.A., Zavarzin, G.A., 1993. *Halocella cellulolytica* gen. Nov., sp. nov., a new Obligately anaerobic, halophilic. Cellulolytic bacterium. Systematic and Applied Microbiology 16, 385–389.
Sinninghe Damsté, J.S., Rijpstra, W.I.C., Hopmans, E.C., Schouten, S., Balk, M., Stams, A. J.M., 2007. Structural characterization of diabolic acid-based tetraester, tetraether and mixed ether/ester, membrane-spanning lipids of bacteria from the order *Thermotogales*. Arch. Microbiol. 188, 629–641.
Sinninghe Damsté, J.S., Rijpstra, W.I.C., Hopmans, E.C., Weijers, J.W.H., Foesel, B.U., Overmann, J., Dedysh, S.N., 2011. 13,16-dimethyl Octacosanedioic acid (iso-diabolic acid), a common membrane-spanning lipid of Acidobacteria subdivisions 1 and 3. Appl. Environ. Microbiol. 77, 4147–4154.
Sinninghe Damsté, J.S., Rijpstra, W.I.C., Foesel, B.U., Huber, K.J., Overmann, J., Nakagawa, S., Kim, J.J., Dunfield, P.F., Dedysh, S.N., Villanueva, L., 2018. An overview of the occurrence of ether- and ester-linked iso-diabolic acid membrane lipids in microbial cultures of the Acidobacteria: implications for brGDGT paleoproxies for temperature and pH. Org. Geochem. 124, 63–76.
Sinninghe Damsté, J.S., Rijpstra, W.I.C., Huber, K.J., Albuquerque, L., Egas, C., Bale, N. J., 2023. Dominance of mixed ether/ester, intact polar membrane lipids in five species of the order *Rubrobacterales*: Another group of bacteria not obeying the "lipid divide.". Syst. Appl. Microbiol. 46, 126404.
Sohlenkamp, C., Geiger, O., 2016. Bacterial membrane lipids: diversity in structures and pathways. FEMS Microbiol. Rev. 40, 133–159.
Sturt, H.F., Summons, R.E., Smith, K., Elvert, M., Hinrichs, K.U., 2004. Intact polar membrane lipids in prokaryotes and sediments deciphered by high-performance liquid chromatography/electrospray ionization multistage mass spectrometry - new biomarkers for biogeochemistry and microbial ecology. Rapid Commun. Mass Spectrom. 18, 617–628.
Suda, Y., Okazaki, F., Hasegawa, Y., Adachi, S., Fukase, K., Kokubo, S., Kuramitsu, S., Kusumoto, S., 2012. Structural characterization of neutral and acidic glycolipids from *Thermus thermophilus* HB8. PLoS One 7, e35067.
Takai, K., Moser, D.P., Onstott, T.C., Spoelstra, N., Pfiffner, S.M., Dohnalkova, A., Fredrickson, J.K., 2001. Alkaliphilus transvaalensis gen. Nov., sp. nov., an extremely alkaliphilic bacterium isolated from a deep south African gold mine. Int. J. Syst. Evol. Microbiol. 51, 1245–1256.
Wiegel, J., Ljungdahl, L.G., 1981. Thermoanaerobacter ethanolicus gen. Nov., spec. Nov., a new, extreme thermophilic, anaerobic bacterium. Arch. Microbiol. 128, 343–348.
Wiegel, J., Braun, M., Gottschalk, G., 1981. Clostridium thermoautotrophicum species novum, a thermophile producing acetate from molecular hydrogen and carbon dioxide. Curr. Microbiol. 5, 255–260.
Yang, Y.-L., Yang, F.-L., Jao, S.-C., Chen, M.-Y., Tsay, S.-S., Zou, W., Wu, S.-H., 2006. Structural elucidation of phosphoglycolipids from strains of the bacterial thermophiles *Thermus* and *Meiothermus*. J. Lipid Res. 47, 1823–1832.
Yang, F.-L., Hua, K.-F., Yang, Y.-L., Zou, W., Chen, Y.-P., Liang, S.-M., Hsu, H.-Y., Wu, S.-H., 2008. TLR-independent induction of human monocyte IL-1 by phosphoglycolipids from thermophilic bacteria. Glycoconj. J. 25, 427–439.